

Characterizations of thermoelectric for energy harvesting on low-level heat sources

A.M. Abdal-Kadhim*, S.L. Kok

Faculty of Electronic and Computer Engineering, Universiti Teknikal Malaysia Melaka,
Hang Tuah Jaya, 76100 Durian Tunggal, Melaka, Malaysia

*Corresponding e-mail: ali.challenger89@yahoo.com

Keywords: Thermal energy harvesting; seebeck effect; low-level heat resources;

ABSTRACT – Electric power harvesting from thermal energy using thermoelectric (TE) has been getting popular as a potential electrical energy source to replace batteries due to its direct current output. The focus of this paper is on the investigation of low level thermal energy below 150 °C that generated from electronic devices and mechanical machinery, and using TE's to convert the heat energy, which normally treated as wasted energy into a useful amount of electrical power to power up portable low power electronic devices. For this study, the TE module is subjected to a range of heat source using heating element that resemble the real temperature that generated from the real electronic devices and mechanical machinery. The quantity of harvested electrical power was reported. From the experimental results it can be observe that the voltage output is linearity proportion to the applied heat gradient on the TE faces. At a temperature gradient of 60 °C, a voltage output of 4 V is measured. The voltage output can be increased by stacking the TE on top of each other, from 0.067V/Δ°C for 1 TE to 0.093V/Δ°C for 4 TE.

1. INTRODUCTION

The latest developments in thermoelectric materials and structures have led to revive the interest in thermal to electrical energy harvesting which presents a new and attractive substitutional solution to the conventional power supplies (batteries). One of the most common method of generating electrical power with the aid of heat is by producing a mechanical movement in turbines, where is considered very old approach. However, this is not the only way of generating electricity power via heat. Therefore, as an alternative to that classical approach, the thermoelectricity generator TEG principle is an emerging technology to be explored along with further development to increase the efficiency and the reliability [1,2]. The TE harvester employing Seebeck effect which it's discovered in 1821 by Tomas Seebeck. This behaviour is described as when heating up one surface of TE element, and cooling down the other surface, will cause to generate an electrical current at the end terminals of the TE element. A TE harvester has shown promising features such as long life cycle, no moving parts needed, simplicity and high reliability. These days, the interest of thermal energy harvesting growing faster and more investigations are moving into its area, where there are some successful industrial applications using TE generators. The Seiko Thermic watch considered the first

application ever of thermal energy harvesting to a consumer product [3]. The wrist watch was driven via a TE module to convert the user body heat into electrical energy. A 22 μW can be harvested by the TE module with about a 1K temperature gradient between the wrist and the environment at room temperature. Moreover, this harvested energy not only drives the watch but also charge a 4.5mAh lithium-ion battery. Other researchers developed a novel ultralow-power management circuit for an autonomous multisensory system for agricultural application where was powered via thermal energy harvester [4]. They succeeded to harvest about 110-mV/°C and also prolog the system lifetime from 136 h to more than 266 h. Dejan Rozgic and Dejan Markovic in [5] present a thin-film array-based thermoelectric energy harvester fabricated in a 0.83cm² footprint along with a power management unit integrated into 65nm CMOS. Their prototype was targeted for biomedical applications where they achieved 645μW regulated output power harvested in-vivo from a rat implanted.

2. LOW-LEVEL HEAT RESOURCES SURVEY

In this paper, a mini survey was conducted to investigate various low-level heat sources that can be categorized as household electrical appliances are presented. This survey was targeted low-level of heat emission (less than 150 °C). These items considered good heat sources for the application of energy harvesting because they are operating almost 24/7.

Hanna (HI93552R) kjt-thermocouple thermometer was the main equipment used to conduct this study. From Figure 1 it can be observed that the tested devices are generally emitting from 40°C in case of laptop charger up to 130°C in case of steam pressure cooker during their operating time. Since the ambient room temperature was measured at about 28°C. Therefore, the delta of temperature for every tested item in the figure can be obtained via "ΔT=Heat Emitted-Room Temperature", which its start from ΔT=18°C up to ΔT=100°C. So according to this data the following experiment and in order to characterize the TE output a ΔT within the range of (5°C to 60 °C) will apply to the TE element.

3. TE HARVESTER CHARACTERIZATIONS SET-UP

In order to characterize the TE output a PCB resistive heater 5.5cm² in size fabricated to simulate a variable heat source. A group of four TE's used here from

Laird xc31 connected in series. A heat sink with 19 cm in diameter and 9 cm in height used to sink out the heat on the other side of TE, Figure 2.

A variable power supply connected to the PCB resistive heater in order to generate a different ΔT within range of (5°C to 60 °C) to the TE under test, and the open circuit V-out was recorded via a digital voltmeter.

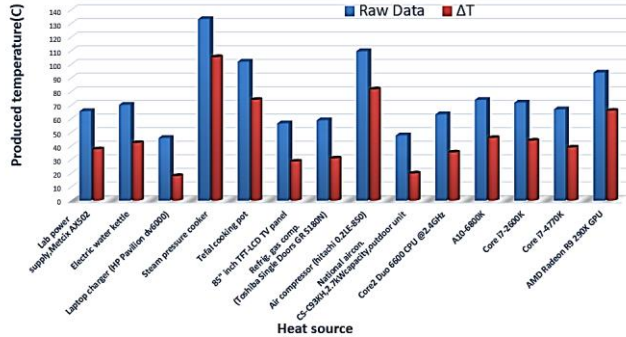


Figure 1 Low-level heat sources and their ΔT at room temperature = 28°C.

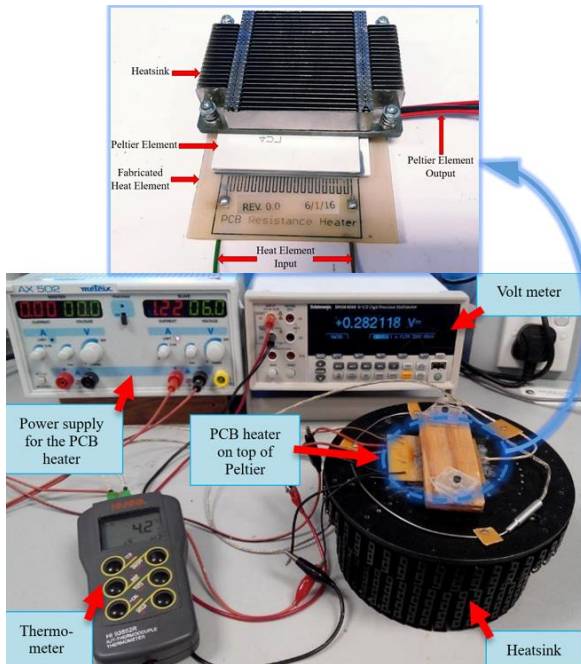


Figure 2 TEG Characterization experimental set-up.

4. EXPERIMENTAL RESULTS AND DISCUSSION

The experiment starts with a single TEG element and then cascaded the rest sequentially by connected their output in series. Whatever using one TEG or more, they all generate about 0.5 DC.V at $\Delta T=5$ °C. Where then the V-out increased with direct proportional manner with ΔT . The maximum output can get from single TEG is 4DC.V at ΔT equal to 60°C. Whereas the maximum output measure of cascading four TEGs recorded is about 5.5 DC.V, Figure 3 illustrates the DC. V-out harvested from multiple TEG at different temperature gradient.

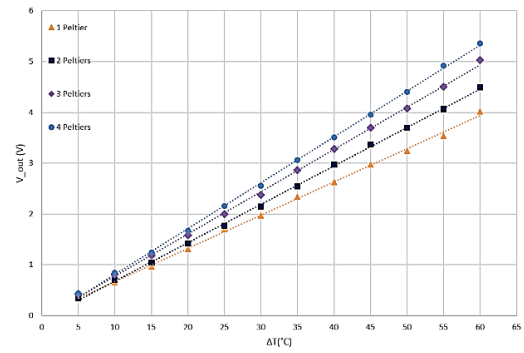


Figure 3 DC. V-out harvested from multiple TEG at different ΔT gradient.

5. CONCLUSION

A mini survey of low-level heat sources has been reported. PCB resistive heater used to apply different temperature gradient to the TEG. From the results can conclude that the increment of the TEG number doesn't have the biggest effect on the V-out as the ΔT . Where at $\Delta T=60$ the V-out will be increased by 0.5 V only with every stacked TEGs.

ACKNOWLEDGEMENT

The authors would like to acknowledge the support of this work by the Malaysian Ministry of Higher Education under the FRGS research grant No. FRGS/2/2014/SG02/FKEKK/02, UTeM ZAMALAH, and UTeM internal grant PJP/2014/FKEKK(1B)/S01293 as well as the facility support by the Faculty and ASECs Research Group, CeTRI, UTeM.

REFERENCES

- [1] F. Attivissimo, A.M.L. Lanzolla, D. Passaghe, M. Paul, D. Gregory and A. Knox, "Photovoltaic-thermoelectric modules: a feasibility study," *IEEE International Instrumentation and Measurement Technology Conference (I2MTC) Proceedings*, 2014.
- [2] C. Bobean and V. Pavel, "The study and modeling of a thermoelectric generator module," in *The 8th International Symposium on Advanced Topics in Electrical Engineering (ATEE)*, 2013.
- [3] M. Kishi, H. Nemoto, T. Hamao, M. Yamamoto, S. Sudou, M. Mandai and S. Yamamoto, "Micro-thermoelectric modules and their application to wristwatches as an energy source," in *International Conference on Thermoelectrics*, 0-7803-545 1 -6, 1999.
- [4] J.P.C. Dias, F.J.O. Morais, M.B. Morais França, E.C. Ferreira, A. Cabot, and J.A.S. Dias, "Autonomous multisensor system powered by a solar thermoelectric energy harvester with ultralow-power management circuit," *IEEE Transactions on Instrumentation and Measurement*, vol. 64, 2015.
- [5] D. Rozgic and D. Markovic, "A 0.78mW/cm² autonomous thermoelectric energy-harvester for biomedical sensors," in *Symposium on VLSI Circuits Digest of Technical Papers*, pp. 278-279, 2015.

Energy conversion: A study on rainfall's gravitational force for urban area power generation

M.F. Yaakub^{1,2,*}, S. Abdullah¹, M.F. Basar^{1,2}, F.H. Mohd Noh³, M.H. Harun^{1,2}, M.F.M.A Halim^{1,2}

¹⁾ Faculty of Engineering Technology, Universiti Teknikal Malaysia Melaka, Hang Tuah Jaya, 76100 Durian Tunggal, Melaka, Malaysia

²⁾ Center for Robotics and Industrial Automation, Universiti Teknikal Malaysia Melaka, Hang Tuah Jaya, 76100 Durian Tunggal, Melaka, Malaysia

³⁾ Faculty of Electronics and Electrical Engineering, Universiti Tun Hussein Onn Malaysia, 86400 Parit Raja, Johor, Malaysia

*Corresponding e-mail: muhamadfaizal@utem.edu.my

Keywords: Pico-hydro; gravitational, rainfall;

ABSTRACT – Demand on energy is increasing in every area in the world. Unstable fossil price, their rapid depletion has led to the intensive research on new energy source and energy conversion. This paper presents the potential study of energy conversion, from gravitational force of a rainfall water to an electrical energy to be used as a power generator in an urban area. Two methods of experimental work (separated and combined generators configuration) have been proposed to verify the potential energy with the implementation of pico-hydro technology. The result shows the promising figure and explained in the paper.

1. INTRODUCTION

In the new millennium era, ever since the electricity was found more than century ago, it has become one of the most valuable commodity. To provide the sufficient electricity with lower cost is a challenge for the year to come especially in urban area. The increases population, a number of skyscrapers, factories, as well as home residence, have made the situation become crucial.

In Malaysia, hydropower plant, gas-based power plant, coal power plant continues to dominate the power generation sectors. However, gas and coal based power plant much depend on the availability and price of the fossil material. Large hydropower plant requires huge capital and land [1]. As a result, this opens an opportunity to a new research in renewable energy and energy conversion field. Pico-hydro technology with a capacity less than 5kW has become popular recently due to its flexibility to be applied in small scale power generation [2].

Geographically, Malaysia is located near to equator which received a huge amount of rain yearly. Peninsular Malaysia and Malaysian Borneo side receive around 2500 mm and 5080mm of rainfall, respectively in average each year [3]. Kuching, Tawau, Kota Bharu, Kuala Lumpur are among the highest receiver of rainfall. Therefore, pico-hydro generation is feasible at these locations with the presence of skyscrapers and other commercial buildings.

Using rainfall and height of skyscrapers as a medium, authors aim to see the potential to generate an energy by converting the gravitational force and water

flow of the rainfall in the pipe to an electrical energy. The case study and experimental work were done in Melaka.

2. METHODOLOGY

The study involved experimental work done at a three-story building located at Faculty of Electrical Engineering. The exercise focused on finding the best configuration to generate higher energy conversion rate. Three pico-hydro generators were used in each experimental. Figure 1 summarized the experimental framework for this research. The First configuration (configuration 1) use all 3 generators in a single experiment whereby second configuration (configuration 2) use one generator at a time. This mean configuration 2 has 3 experimental work for different generator location. Figure 2 illustrates the experimental setup for configuration 1 and configuration 2.

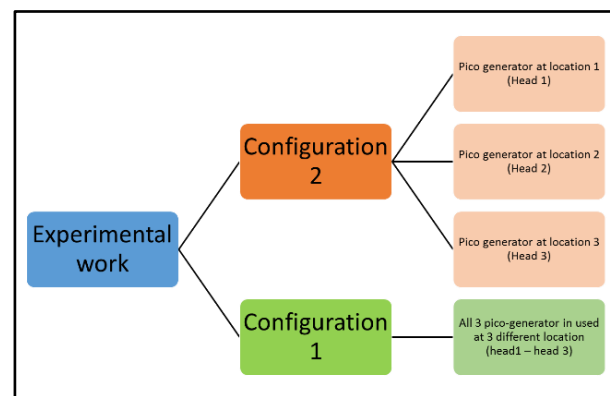


Figure 1 Experimental Framework for the research.

The amount of output power produced is depended on the vertical drop of water flow (H) in the pipeline and the water flow rate (Q) [4-5].

$$P = Q \cdot H \cdot \rho \cdot g \quad (1)$$

where,

P = Potential Power (watts)

Q = Volumetric flowrate (litre/sec)

H = gross head (m)

ρ = water density (kg/m³)

g = gravitational constant (9.81 m/s²)

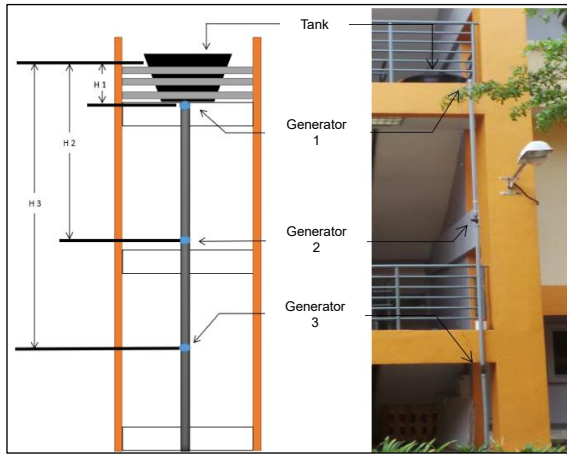


Figure 2 Experimental Setup for configuration 1 and 2.

The power equation is then modified by an efficiency factor (η):

$$P = Q \times H \times g \times \rho \times \eta \quad (2)$$

where,
 $\eta = \text{efficiency}$

The aforementioned equation is necessary to provide a reasonable estimation of output power to be produced by the system regardless of its generator size and rating.

3. RESULTS AND DISCUSSION

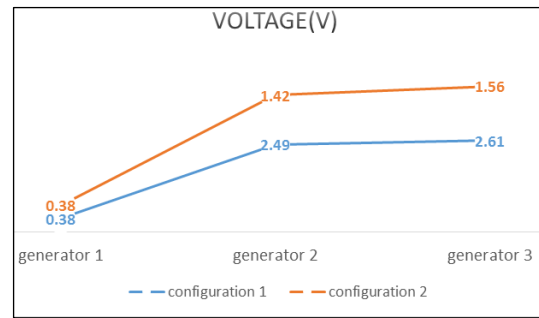
The outcome of the experimental work are illustrated in Figure 3 (a), (b) and (c). Figure 3 portrays the comparison result of configuration 1 and configuration 2 in term of voltage, current, and power generated from the energy conversion work. Higher energy conversion efficiency can be achieved with correct placement of generator depends on head and flow density of the water. Clearly seen that configuration 2 provides fewer energy losses after the conversion. With 3 generators placed at the same time, losses (i.e. frictions, trash rack, entrance losses) will become bold and affect the conversion.

4. CONCLUSION

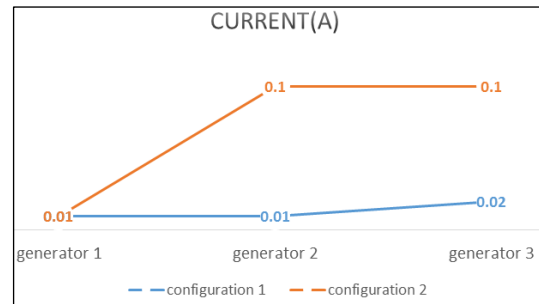
As a conclusion, it should be noted that there is a big potential to acquire an energy from the gravitational force of the rainfall with an appropriate apparatus and method. With the proposed method, clearly that the energy conversion is feasible with the presence of skyscrapers in an urban area. With a right placement of generator at an optimum head distance, the maximum efficiency of energy conversion rate can be tremendously obtained, in this case, 736.51% (in mWatt). Pico-hydro implementation in the research contributes to the cost efficient due to its small in size, environmentally friendly, and hassle-free maintenance.

ACKNOWLEDGEMENT

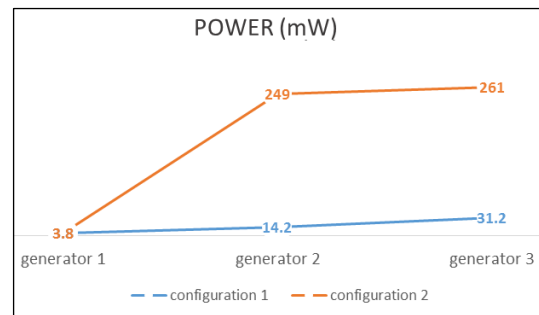
The authors appreciate the support granted (PJP/2016/FTK-CERIA/S01492) by Universiti Teknikal Malaysia Melaka (UTeM) in pursuing this research.



(a)



(b)



(c)

Figure 3 Outcome of the experimental work (configuration 1 vs configuration 2) of (a) output voltage, (b) output current and (c) output power.

REFERENCES

- [1] S.S. Katre and V. N. Bapat, "Induction generator for Pico-hydro generation as a renewable energy source," *2015 International Conference on Energy Systems and Applications, Pune*, pp. 130-134, 2015.
- [2] M.F. Basar, A. Ahmad, N. Hasim and K. Sopian, "Introduction to the pico hydro power and the status of implementation in Malaysia," *2011 IEEE Student Conference on Research and Development, Cyberjaya*, pp. 283-288, 2011
- [3] C.L. Wong, R. Venneker, S. Uhlenbrook, A.B.M. Jamil, and Y. Zhou. "Variability of rainfall in Peninsular Malaysia," *Hydrology and Earth System Sciences Discussions* 6, no. 4, 5471-5503, 2009.
- [4] K. Sopian, and J.A. Razak, "Pico hydro: Clean power from small streams," *Proceedings of the 3RD WSEAS International Conference On Energy Planning, Saving, Environmental Education, EPESE '09, Renewable Energy Sources, RES '09*, pp. 414- 419, 2009.

Off-grid photovoltaic automated river debris collector system

I.M. Saadon^{1,2,*}, J.H. Hassanudin¹, N. Norddin^{1,2}, W. H. W. Hassan¹

¹⁾ Faculty of Engineering Technology, Universiti Teknikal Malaysia Melaka,
Hang Tuah Jaya, 76100 Durian Tunggal, Melaka, Malaysia

²⁾ Centre for Robotics and Industrial Automation, Universiti Teknikal Malaysia Melaka,
Hang Tuah Jaya, 76100 Durian Tunggal, Melaka, Malaysia

*Corresponding e-mail: mastura@utem.edu.my

Keywords: Off-grid photovoltaic, AC water pump, debris management

ABSTRACT – Based on monitoring conducted by Department of Environment Malaysia (DOE) in 2013, 341 out of 473 rivers in Malaysia were found polluted. In this paper, a system of river debris collector using a stand-alone photovoltaic is presented. The photovoltaic module is sized to power up an AC water pump and Arduino microcontroller which is embedded to a distance sensor to automate the system. The prototype involves a water wheel, conveyor belt and dumpster barge. The debris collecting system is expected to be turned on for two hours daily to clean the river.

1. INTRODUCTION

River pollution may contain many types of disease-causing organism. It affects the ecosystem and living organism in the river. Sewage system even making it worst. Moreover, debris floated on the river is problematic to clean. In this project, a photovoltaic (PV) powered water pump system is developed by off-grid photovoltaic system sizing. A prototype that is built using a water wheel, conveyor belt and dumpster barge is developed to run the system. It uses renewable energy for promoting environmental friendly technology in line with Malacca city slogan; City of Green Technology.

Figure 1 shows a SketchUp drawing of the river debris collector system. The concept design of this system includes the parts no 1-8 shown in the figure. The system is designed to float on the river. The PV used is from mono-crystalline silicon that has the highest efficiency compared to others. The PV modules must be slanted at optimum angles so as to collect the maximum solar energy available in a specific region [1]. The orientation and the tilt of a solar panel strongly affect the amount of the collected yield. In Malaysia, tilt angle during dry season is 0° [2].

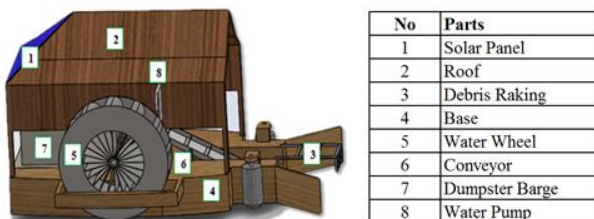


Figure 1 SketchUp design of automated river debris collector system.

2. METHODOLOGY

Figure 2 indicates the operation block diagram of the system. The ac water pump is powered by DC 12V battery through the charger controller and a 60W 12V-230V power inverter. The battery stores electrical energy produced by module during the day time and delivers it during cloudy days. A deep cycle battery is used in PV system as it is maintenance free, low price and have longer life span [3]. PWM type of charger controller is chosen; considering that MPTT type has excellent efficiency in charging but it is costly. The water pump is used to eject water jet to run the water wheel and creates water flow that attracts debris towards the system. The volume flow rate should be high to create water flow. When the water wheel rotates, it moves the conveyor belt that carries the debris into the automatic dumpster barge that is equipped with a distance sensor on top of it to detect the debris height. The sensor measures with analog signal ranges between a values of 0 to 1023 when observed by Arduino serial monitor. When the height reaches its maximum, the water pump will stop automatically to avoid debris overflow. In this condition, it will stop the movement of water wheel and conveyor belt as well.

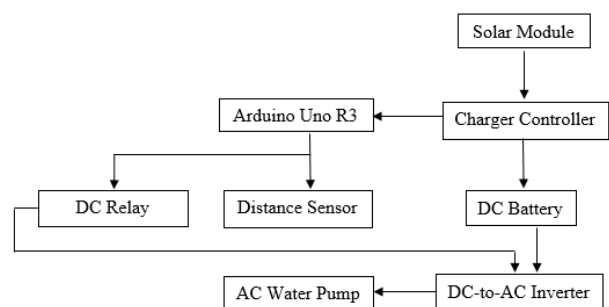


Figure 2 System block diagram.

The PV system sizing is determined based on the load size and the daily usage. Equation (1) is used to determine the size of PV module and battery capacity sizing is determined using Equation (2). By summing the load from water pump and Arduino, the total load is 120Wh/day. Considering peak sun hour (PSH) is 4 hours with 0.7 performance ratio (Pr), the value of peak power is 42.86Wp. Hence, a 50W 12V monocrystalline PV module with a 12V 10AH deep cycle battery are used for this system.

$$(Wp = Wh / (PSH \times Pr)) \quad (1)$$

$$(I = \div Wh / V) \quad (2)$$

Equation 3 is used to determine how long the battery can last to run the system. The value of Ampere – Hour rating and continuous current is 10Ah and 5A respectively. The period of discharge time is 2 hours.

$$\text{Continuous current (A)} = \frac{\text{Ampere-Hour Rating}}{\text{charge/discharge time}} \quad (3)$$

3. RESULTS AND DISCUSSION

The PV module is tested from 9.00am to 5.00pm with 30° tilt. Figure 3 and Figure 4 show the irradiance and temperature effect on voltage. Irradiance and temperature is low in the early morning and increases as the sun rises, causing the voltage to increase. The highest recorded irradiance is 1031 W/m² at 1.00 pm, and temperature is 61.5 °C at 12.00 pm which is the peak time to obtain high irradiance especially when the sky is cloudless. The voltage remains high which is ~12V until 5pm.

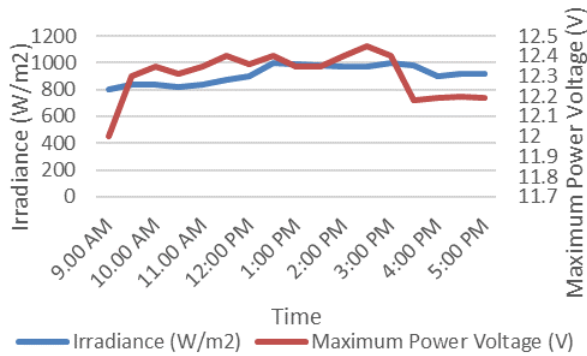


Figure 3 Relationship between irradiance and maximum power voltage.

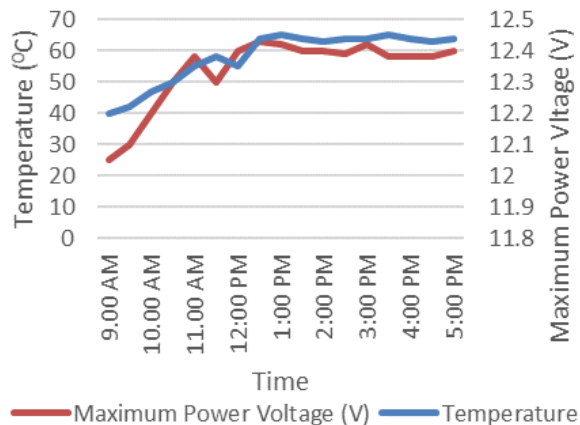


Figure 4 Relationship between temperature and maximum power voltage.

The data taken for electric current that flows in the conductor is shown in Table 1. Based on Equation (3), the current required to charge the battery in 8 hours is 1.25A. From this data, it can be concluded that the battery is able to be charged within 8 hours.

The battery charging time is tested from 9.00am until 5.00pm. The voltage increases steadily and is fully charged at 3.00pm as shown in Figure 5.

Table 1 Radiation vs Current

Time	Irradiance, (W/m ²)	Power Current, (Imp)
9.00am	810	1.26
11.00am	891	1.33
1.00pm	1030	1.46
3.00pm	965	1.32
5.00pm	943	1.27

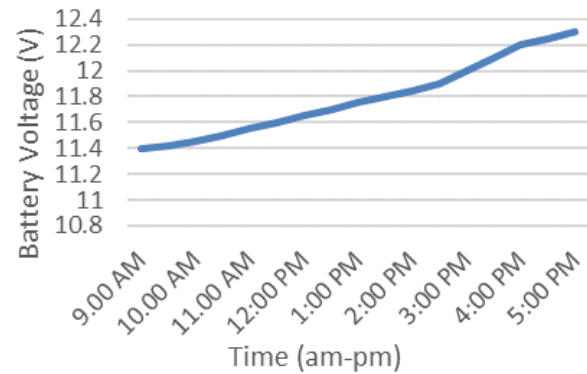


Figure 5 Battery charging time.

4. CONCLUSION

The prototype as presented in this paper is able to generate renewable energy to supply to the system. Automatic river debris management system is very important and should be placed at all rivers because it is environmentally safe and reduce man power. This system can be potentially developed into a larger scale, by considering a higher power for the water pump.

5. ACKNOWLEDGEMENT

The authors would like to express deep appreciations to the Ministry of Higher Education Malaysia and Universiti Teknikal Malaysia Melaka (UTeM) for providing a PJP grant (PJP/2015/FTK(9A)/S01414), opportunity and necessary facilities to support this work.

REFERENCES

- [1] T. Khatib, A. Mohamed, K. Sopian, "A review of solar energy modeling techniques," *Renewable and Sustainable Energy Reviews*, vol. 16, pp. 2864-2869, 2012.
- [2] T. Khatib, A. Mohamed, K. Sopian, "Optimal sizing of hybrid PV/wind systems for Malaysia using loss of load probability," *Energy Sources, Part A: Recovery, Utilization, and Environmental Effects*, vol. 37, pp. 606-613, 2015.
- [3] A. Pradhan, S. M. Ali and P. Behera, "utilisation of battery bank for solar PV system and classification of various storage batteries," *International Journal of Science and Research Publications*, vol. 2, pp. 1-5, 2012.

Performance analysis of dual-axis solar tracker

S. Ahmad^{1,*}, M.C. Koo¹, A. Noordin¹, S.H. Johari¹, S.H. Mohamad¹, A.S. Sadun²

¹) Faculty of Engineering Technology, Universiti Teknikal Malaysia Melaka,
Hang Tuah Jaya, 76100 Durian Tunggal, Melaka, Malaysia

²) Faculty of Engineering Technology, Universiti Tun Hussein Onn Malaysia,
86400 Parit Raja, Johor, Malaysia

*Corresponding e-mail: suziana@utem.edu.my

Keywords: Energy conversion; solar tracker

ABSTRACT –Among the natural energy, solar is one the energy in which adoptable and famous to generate electricity. This project proposed a solar tracker that able to increase energy harvest from the sun with dual-axis tracking system. The project purposely to design mechanism structure and analyze the power output of a tracker. The tracker consists of a controller unit with motors, sensor and energy storage. The solar tracking system facing to the sun in azimuth and altitude during daytime more comparing to static solar system. In comparison, an output power of tracker solar panel and a fixed solar panel are presented.

1. INTRODUCTION

Global warming and pollutions happen as serious issues because of the developments. In order to overcome these global issues, one of the ways is replacing the non-renewable energy with renewable energy to avoid the produce of harmful wastes. The common renewable energies are source from natural, such as wind energy, hydraulics energy, heat and solar energy. Solar energy or known as photovoltaic (PV) is a technology that involves the direct conversion of solar radiation from the sun into electricity using solar cells and is based on the photovoltaic effect.

Progress and development of the PV systems are increasing in all around the countries. IEA-PVPS in A Snapshot of Global PV 1992-2012 has reported that a cumulative PV installation in 23 IEA-PVPS countries is 89.5 GW [1]. Photovoltaic system does not need broad technological base but more research has been done to maximize the electricity generation from PV system. These research including studies on new material of solar cell, maximum power point tracker and solar tracking [2].

Many methods have been proposed to maximum electricity energy generation by using solar tracking system. The tracking solar system will move the solar panel accordingly to the sun radiation. The movement based on dual-axis or single axis mechanism. The single-axis solar tracker is implemented to change in azimuth (horizontal) angle while the dual-axis solar tracker is moved in both azimuth (horizontal) and altitude (vertical) angle [3]. In previous studies, a solar panel with tracking system produces more electricity compare to static solar panel [2-4]

2. A DUAL-AXIS SOLAR TRACKER

The ideas of this project basically are maximizing the output power generated from solar by solar tracking system then combine with energy storage. Arduino UNO board will be used as the control unit central for the whole system of the project. The direct current stepper motor attaches with mechanical work with sensing unit the system, combine with sensing unit to perform the tracking system. Figure 1 below is the idea of this project with a simple block diagram.

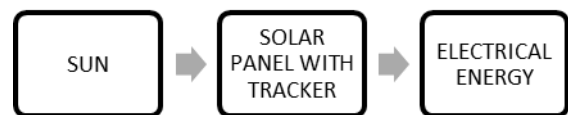


Figure 1 A solar tracker.

An idea should always have a design before authenticate it and develop into a product. Therefore, a solar tracker is designed as shown in Figure 2. The actual prototype is developed and constructed based on the design drawing. The tracker is connected to controller unit and battery as a storage unit.

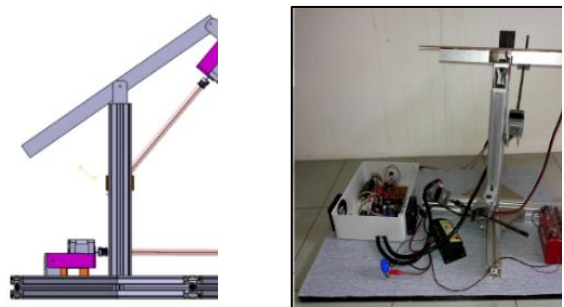


Figure 2 Prototype of a solar tracker.

Light sensing unit is one of the important parts of input for this tracking system. Through the light sensing unit, it detects lights, and sending the signal to the controlling unit, the system then moves toward the direction where light detected. Figure 3 shows light sensing unit and four LDRs needed to detect all angle direction of the sun's radiation.

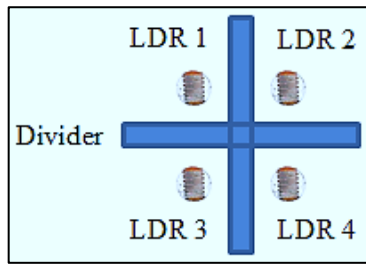


Figure 3 Design of light sensing unit.

Table 1 is the list of specification and dimension. The specification solar panel power used in prototype is 10 watts, with maximum generating Voltage 20 Volts and Current 650 mili-Amps

Table 1 Prototype specification.

Specification	Dimension (cm)
Height	44
Cross Base Length	48
Solar Panel Frame Length	38
Solar Panel Frame Width	33

3. RESULTS AND DISCUSSION

The development of this process is focusing on energy generated and angle of tracker movement. The angle produced is measured on the Portable Dual Axis Solar Tracking System. It is using the Acceleration and Gyro sensor to detect the oscillated angle then display on the LCDs. Figure 4 and Figure 5 are showing the angle oscillated in both Y and X axis every hour respectively.

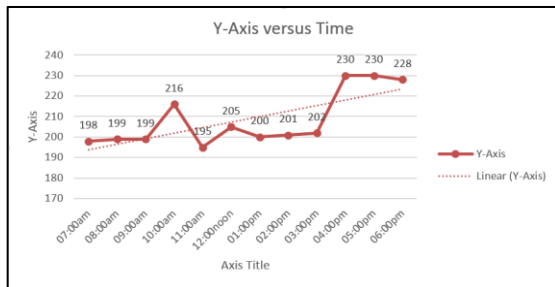


Figure 4 Y-axis (angle) versus time.

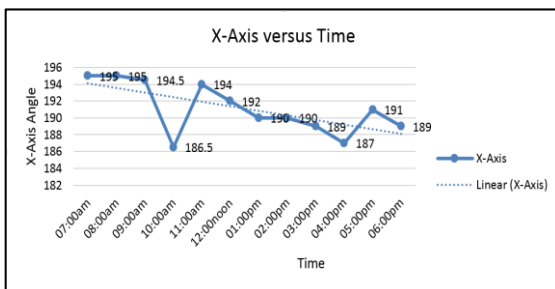


Figure 5 X-axis (angle) versus time.

The data are average from several days in different weeks. Thus, position implant may affect the angle detected.

The energy generated from both solar tracking system and fixed solar panel are measured in Voltage (V) and Current (A) by using digital multi-meter. From the data, the Power (W) produced are calculated. Figure 6 shows the comparison between portable dual axis solar tracking system and fixed panel in term on Power (Watt). A tracker solar panel produces 7.05Wh meanwhile fixed solar panel produced 4.92Wh. The efficiency for solar tracker and fixed panel is 67.81% and 47.38% respectively.

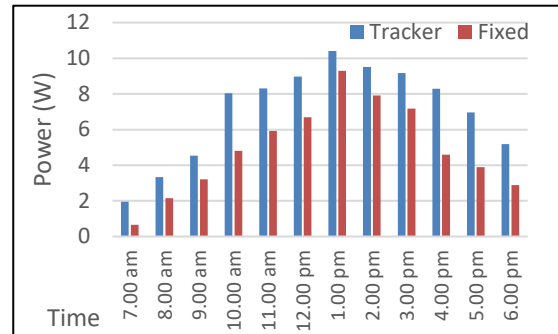


Figure 6 Power gain over time.

4. CONCLUSION

As conclusion, undeniable, solar panel with sensing unit on tracking mechanism is the way to improve the efficiency of solar panel in generating energy from sun. The light sensing unit successfully leads the mechanism Dual-Axis Solar Tracking System face parallel toward the sun. When the light sensing unit detect the sun position is changed away from parallel position, Arduino microcontroller will receive the signal and trigger the stepper motors to move until the position where parallel with sun. This combination is success to meet the objective. A solar tracking system is having higher efficiency compared to fixed static solar panel

ACKNOWLEDGEMENT

The authors would like to thanks Universiti Teknikal Malaysia Melaka (UTeM) and Faculty of Electrical Technology for supporting this project.

REFERENCES

- [1] Agency, I.E., PVPS Report - A Snapshot of Global PV - 1992-2012 <http://www.iea-pvps.org/>, 2013.
- [2] J.F. Lee and N.A. Rahim, "Performance comparison of dual-axis solar tracker vs static solar system in Malaysia," 2013 *IEEE Conference on Clean Energy and Technology (CEAT)*, Langkawi, pp. 102-107, 2013.
- [3] P. Bajpai and S. Kumar, "Design, development and performance test of an automatic two-axis solar tracker system," *India Conference (ICoN)* West Bengal, India. IEEE, pp. 1-6, 2011.
- [4] S. Ahmad, S. Shafie and, M.Z.A. Ab Kadir, "A high power generation, low power consumption solar tracker," *IEEE International Conference on Power and Energy (PECon)*, pp. 366-371, 2012.

Thermogravimetric analysis of palm shell solid waste

H. Ghafar^{1,*}, R. Zailani², M.A.A. Hamid Pahmi¹, S.N.A.M. Halidi¹, A.S. Abdullah¹, A.F.M. Yamin¹

¹) Faculty of Mechanical Engineering, Universiti Teknologi MARA,
Jalan Permatang Pauh, 13500 Permatang Pauh, Pulau Pinang, Malaysia

²) Faculty of Mechanical Engineering, Universiti Teknologi MARA Shah Alam, Selangor, Malaysia

*Corresponding e-mail: halim4346@ppinang.uitm.edu.my

Keywords: Biomass; palm shell; thermogravimetric analysis

ABSTRACT – Being a major contributor to biomass industry, oil palm is recognized as one of the resources in developing countries like Malaysia. Thermogravimetric analysis (TGA) is conducted to observe the contents of the palm shell. By using TGA, thermal characteristics of palm shell is studied. It is found that palm shell contains volatile matter, fixed carbon, ash and also moisture. Volatile matter contributes significantly to the contents of palm shell at about 55.64%. Fixed carbon and ash contributes 32.64% and moisture content contributes 12%. These observed values proved that the palm shell can be used as one of the resources for biomass energy.

Table 1 Types of renewable energy in Malaysia and its energy value [1].

Renewable Energy Sources	Energy value in RM Million (annual)
Forest Residues	11984
Oil Palm Biomass	6379
Solar Thermal	3023
Mill Residues	836
Hydro	506
Solar PV	378
Municipal Waste	190
Rice Husk	77
Landfill Gas	4

1. INTRODUCTION

Oil palm is recognized as one of biomass resource and can be found in normally in developing country such as Malaysia. Oil Palm is widely planted in Malaysia and generates income of estimated RM 6379 million annually and become the second's biggest renewable energy value to Malaysia [1] as shown in Table 1. Its residue consists of empty fruit bunch, fibre and shell. Shell has the highest calorific value, 18,836 kJ/kg compare to empty fruit bunch and fibre which is 6028 kJ/ and 11,344 kJ/kg respectively [2]. The shell has a potential to be used as fuel resource for other applications such as cooking etc. This can be achieved by converting it into more useful energy such as solid fuel and biofuel by number of ways such as pyrolysis, gasification, etc.

During the Thermogravimetric Analysis (TGA) of palm shell, moisture content vaporizes at 100 °C. The proportion of cellulose, hemicellulose and lignin very important in determining the suitable thermal conversion process, such as pyrolysis, gasification, etc. The biodegradability of cellulose/hemicellulose is higher than lignin. Lignin forms mainly char while cellulose and hemicellulose form mainly volatile products.

The objective of this paper is to study on the thermal characteristics of palm shell using thermogravimetric analysis.

2. METHODOLOGY

Sample of palm shell were obtained from palm oil mill at Kluang, Johor. The samples were then dried in the oven at 50°C. for 24 hours. The dried samples were grounded into powder using crusher. Proximate analysis was conducted using Thermogravimetric Analysis (TGA) method.

TGA method was used to analyze the content and thermal characteristics of oil palm. TGA was performed on TGA analyzer model Pyris1 as shown in Fig 1. The grounded samples of weight 20 mg were placed in the cup and was heated at the rate of 10K/min from a room temperature to 800 °C. It was conducted according to ASTM D 5865-11a [5].



Figure 1 TGA analyser.

3. RESULTS AND DISCUSSION

Figure 2 show the thermogravimetric analysis result for palm shell solid waste. Thermogravimetric (TG) profile provides thermal characteristics of biomass as a result of thermal degradation of its key elements such as hemicelluloses, cellulose and lignin. From the result of palm shell TG profile as shown in Figure 2, initial 11.23% weight loss of palm shell can be observed at about 130°C. This phenomenon was attributed to moisture loss of palm shell. Later on, another significant weight loss by 55.64% due to decomposition of biomass was occurred at up to 530°C due to decomposition of biomass. The devolatilisation occurred at this stage, initiated at about 200°C and completed at about 530°C. This leaves 33.13% residue as the remainder which consist of fixed carbon and ash.

From DTG curve, palm shells devolatilisation shows 2 peaks which represent 2 groups of reaction. The first stage of devolatilization was occurred from 200°C - 320°C and the peak rate of devolatilisation appeared at 280°C, at a rate of 4.4 %/min. The second stage of devolatilization was occurred within temperature range of 320°C to 420°C. The highest peak of the second stage was noticed at 360°C, at a rate of 6.4%/min. The first group of devolatilisation was due to decomposition of hemicellulose and the second group was due to the decomposition of cellulose. It has been reported by other researcher that hemicellulose decomposition at temperature range of 220°C to 300°C, cellulose was decomposition at temperature range of 300°C to 340°C, lignin decomposition was at temperature more than 340°C [6].

Initial weight loss of palm oil was 7.41% at 130 °C as shown in Figure 2. This initial weight loss indicated the moisture loss of the biomass. Afterward, maximum weight loss was observed at temperature range 180°C - 460 °C.

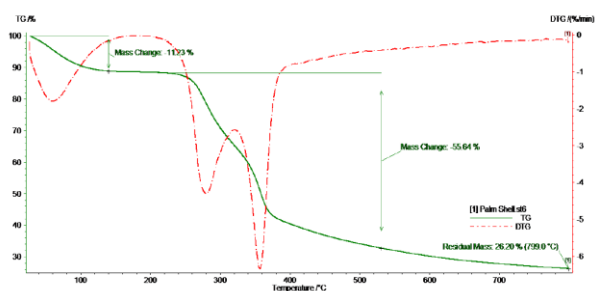


Figure 2 Thermogravimetric analysis of palm shell solid waste.

Based on Table 2, it is observed from proximate analysis that palm shell contains volatile matter, fixed carbon and ash, and moisture. Volatile matter contributes significantly in the content, i.e. 55.64 %. This is followed by fixed carbon and ash at 32.64% and moisture at 12.00%. The same pattern was also observed by previous studies [7].

Table 2 Comparison between values obtain from the experiment and from previous studies.

Proximate analysis	Palm Shell	*Ref. Value
Volatile matter	55.64	67
Fixed carbon and ash	32.64	22.3
Moisture	12.00	9.7

*Source [5].

4. CONCLUSIONS

In conclusion, the values obtained from TGA are in parallel with the one from previous studies. Volatile matter contributes 55.64% to the total content in palm shell. Fixed carbon and ash contributes 32.64% while moisture contributes 12%. Higher content of volatile matter contributes to better production of biofuel. Fixed carbon contributes to the production of solid fuels. Thus, it could be concluded that palm shell is suitable to be used for the production of biofuel due to its higher volatiles matter.

ACKNOWLEDGEMENT

The financial support from MOHE through The Research Management Institute, Universiti Teknologi MARA Malaysia, FRGS (600-RMI/ST/FRGS 5/3Fst(89/2010), is highly appreciated.

REFERENCES

- [1] S. Sumathi, S.P. Chai and A.R. Mohamed, "Utilization of oil palm as a source of renewable energy in Malaysia," *Renewable and Sustainable Energy Reviews*, vol. 12, pp. 2404-2421, 2008.
- [2] S. Mekhilef, R. Saidur, A. Safari and W.E.S.B. Mustaffa, "Biomass energy in Malaysia: Current state and prospects," *Renewable and Sustainable Energy Reviews*, vol. 15, pp. 3360-3370, 2011.
- [3] P. McKendry, "Energy production from biomass (part 1): overview of biomass," *Bioresource Technology*, vol. 83, no. 1, pp. 37-46, 2002.
- [4] E. Apaydin-Varol, E. Pütün and A.E. Pütün, "Slow pyrolysis of pistachio shell," *Fuel*, vol. 86, pp. 1892-1899, 2007.
- [5] Standard Test Method for Gross Calorific Value of Coal and Coke, ed: ASTM International, 1999.
- [6] H. Yang, R. Yan, D.T. Liang, H. Chen and C. Zheng, "Pyrolysis of palm oil wastes for biofuel production," *Asian Journal on Energy and Environment*, vol. 7, pp. 315-323, 2006.
- [7] A. Hussain, F.N. Ani, A.N. Darus and Z. Ahmed, "Thermogravimetric and thermochemical studies of Malaysian oil palm shell waste," *Journal Teknologi*, vol. 45, pp. 43-53, 2006.

Low cost natural convection solar dryer for drying durian tree wood

A. Ngah Nasaruddin^{1,*}, J. Ab Razak^{1,2}

¹⁾ Faculty of Mechanical Engineering, Universiti Teknikal Malaysia Melaka,
Hang Tuah Jaya, 76100 Durian Tunggal, Melaka, Malaysia

²⁾ Centre for Advanced Research on Energy, Universiti Teknikal Malaysia Melaka,
Hang Tuah Jaya, 76100 Durian Tunggal, Melaka, Malaysia

*Corresponding e-mail: afiqah_ngahn@yahoo.com

Keywords: Energy; moisture content; solar dryer

ABSTRACT – This paper presents the study on development of natural convection solar dryer for drying durian tree wood. Currently the wood is dried using open sun drying method. The process is slow and usually interrupted by rain. This study will provide an alternative solution for this problem with a low cost, fast drying, reliable and efficient solar dryer. Due to unpredicted weather condition in Malaysia, the dryer is tested during sunny and cloudy days. The drying time is cut by almost 2 hours. The techno-economy analysis of the solar dryer provides a return of investment (ROI) of 42% which is promising in the field of solar energy application.

1. INTRODUCTION

The aim of drying of agricultural product is to remove moisture so that it can be processed safely to a desired product. In Malaysia, due to hot and humid weather, wood condition can deteriorate so quick which will reduce its service life. It needs a careful treatment to ensure it is thoroughly dried before it can be used for other purpose, i.e. furniture and home accessories. Current method of drying, using open sun drying method, is not suitable for mass production. This method takes a long duration of time and requires close supervision due to weather condition. Therefore, a sheltered drying compartment where the agricultural product can be dried and safely stored will be of more convenient for wood treatment. Stream of air is heated by solar energy can reduce its relative humidity which is then can be used to dry durian tree wood. This form of solar drying approach was expected to improve the quality of the product to be dried, reduce contamination and speed up drying process thus, achieving better quality control and reduction in time taken for drying.

However, the low solar energy density and tropical weather conditions are the major stumbling blocks in identifying suitable application using solar energy as the heat source [1]. Besides that, inappropriate dryer design due to the choice of construction materials, inadequate understanding of the operation of solar dryers and lack of design procedures contribute to poor performance of natural convection type of solar dryer [2].

2. METHODOLOGY

The evaluation of performance for solar dryer was performed by having numbers of wet sample of durian tree wood dried in the drying chamber that equipped with solar collector which provide hot air that passing through

the collector directly to the drying chamber. The wood is having the dimension of 0.28 m x 0.39 m with 0.8 mm thickness. The simulation was carried out using ANSYS software to obtained the information such as the temperature distribution and the air flow inside the system using viscous, k-epsilon and standard wall function model parameter setting.

The analysis includes the on-site measurement and testing of the solar dryer using instrument to capture data on parameters such as wind speed, ambient temperature and relative humidity. All this data obtained will be used to accurately calculate the energy obtained from the drying system and the energy losses from the dryer. Heat transfer equations used in this study are derived from Papade and Boda [3], Cengel and Ghajar [4], and Twidell *et al.* [5].

The individual thermal resistance taken into consideration consists of conduction resistance and convection resistance, which represent the thermal resistance of the wall against heat conduction and the thermal resistance of the surface against heat convection respectively. The total heat transfer for the solar collector can be determined from the summation of the heat transfers through each of layer of the wall.

Total heat transfer, Q :

$$Q_{total} = (T_{\infty 1} - T_{\infty 2}) / R_{total} \quad (1)$$

where

$$R_{total} = L/kA + 1/hA \quad (2)$$

Complete analysis of internal heat transfer in an air heater is however complicated since it involved the same molecule that carries the useful heat and the convective heat loss [5]. The following variables are to be calculated:

- Mass of water to be evaporated, m_w
- Energy required for evaporating water, E_p
- Energy gain by air from radiation, E_a
- Average drying rate, M_{dr}
- Mass flow rate of air, m_a
- Velocity of air, v_a (m/s)

The ideal value of useful heat shows a promising ideal condition the system might be obtained despite the fluctuation of temperature and other parameter that affected the efficiency of the overall system.

i) Collector efficiency:

$$\eta_c = \rho c Q (T_2 - T_1) / G_c A \quad (3)$$

ii) Useful heat flow from solar air collector:

$$P_u = \rho c Q (T_2 - T_1) \quad (4)$$

3. RESULTS AND DISCUSSION

Figures 1 and 2 show the temperature distribution contour of solar collector and the velocity streamline representation for drying chamber respectively. The maximum temperature achieved at solar collector is as high as 94°C. In drying chamber, the instantaneous fluid velocity is the highest at the inlet and outlet of the drying chamber, approximately in the range of 0.023 m/s. The sudden drop in instantaneous velocity can be observed as the air flow hit the durian's wood and it keep on dropping as it flows to the next level of the wood's rack.

Experiments (Figure 3) were conducted to test two different weather conditions; sunny and cloudy. The black paint applied at the wall surface of the drying chamber is black epoxy paint having emissivity coefficient of 0.89. The ambient temperature, average humidity, average wind speed was recorded using an picodata logger, thermocouple and velocicalc-plus. On sunny day, the maximum temperature recorded at the solar collector is 74°C while the maximum temperature at the absorber is 60°C.

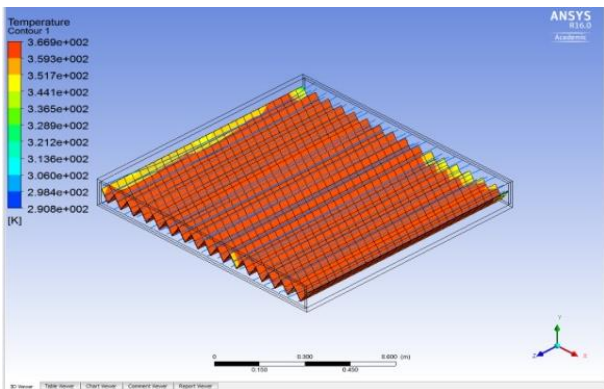


Figure 1 Temperature distribution contour of solar collector.

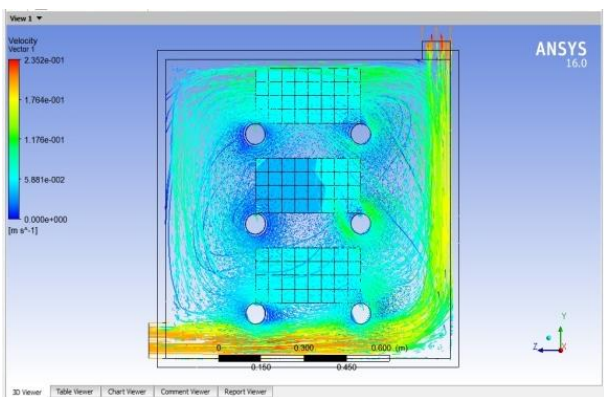


Figure 2 Velocity streamline representation side view for drying chamber.

The capital cost for the development of each unit of solar dryer is RM 240. For a batch of 55 wood trays the profit obtained was RM 577.50. However, with the implementation of eight unit of solar dryer the production increased to 92 wood trays per batch with profit of RM 966.00. In term of return of investment (ROI) which

measure the amount of return on an investment relative to the investment's cost it is resulted with 42% ROI. With respect of the gain from and cost of investment are RM 2719.50 and RM 1920.00 respectively.



Figure 3 Drying process using solar dryer.

4. CONCLUSION

Malaysia had benefited from a weather condition of hot and humid throughout the year. Somehow lead to potential for development of high efficiency solar dryer. Manipulating the abundant energy from the sun for the purpose of drying with less cost involve for constructing is somehow favorable in this case study. On the other hand, the bright side of fully enclose solar dryer is the agricultural product inside the dryer does not need to be monitored frequently from pest attack or the sudden rain compared with open sun drying method. In term of the time taken to dried thin layer of durian tree wood, it only takes approximately 2 hours and 20 minutes compared to 4 hours for conventional open sun drying method. In addition, the designated dryer in the case study can also be used to dry other agricultural product such as rice, tobacco leaves and other relevant crops.

REFERENCES

- [1] M.U. Ude, S.A. Ogunjobi, B.I. Onyia and L.I. Ezigbo, "Drying of millet using solar dryer," *International Journal of Advanced Engineering Research and Science*, vol. 3, pp.1-4, 2016.
- [2] C.A. Komolafe, I.O. Ogunleye and A.O.D. Adejumo, "Design and fabrication of a convective fish dryer," *The Pacific Journal of Science and Technology*, vol. 12, pp. 89- 97, 2011.
- [3] C.V. Papade and M.A. Boda, "Design and development of indirect type solar dryer with energy storing material," *International Journal of Innovative Research in Advanced Engineering*, vol. 1, no. 12, pp. 109- 114, 2014.
- [4] Y.A. Cengel and A.J. Ghajar A.J., Heat and Mass Transfer: Fundamental and Applications. 4th Edition, McGraw-hill Education, 2011
- [5] J. Twidell and T. Weir, Renewable Energy Resources, Taylor & Francis Group 2nd edition, pp 148, 2006.

Analysis of portable temperature-controlled device by using peltier effect

S. Ahmad*, M.E.S. Abdullah, M.F. Yaakub, A.Z. Jidin, S.H. Johari, M. Zahari

Faculty of Engineering Technology, Universiti Teknikal Malaysia Melaka,
Hang Tuah Jaya, 76100 Durian Tunggal, Melaka, Malaysia

*Corresponding e-mail: suziana@utem.edu.my

Keywords: Energy conversion; peltier effect

ABSTRACT –In the era of globalization, the use of products that generate cold and hot temperatures are widely used. The project proposed a portable temperature-controlled Peltier device with a controller. The objectives of project are to develop temperature-controlled device by using Peltier effect and to analyze its performance. A battery, controller unit and a heat sink are used as the main components for a portable temperature controlled device. Set point of 20°C and 40°C are set for cooling and heating process. The result of the project is presented in this paper.

1. INTRODUCTION

With the growth of technologies and development, the demands of electrical energy for daily activities increased. Oppositely, the fossil fuel used for producing electricities dwindling day by day. Besides, environmental pollution also become worst then before. Therefore, thermoelectric material has been studies widely. Thermoelectric involves energy conversion between thermal and electrical energy and heating and cooling material as well as generates electricity [1].

The Peltier effect occurs when DC current carry different amounts of electrical energy in difference conductors and effect significantly in thermoelectric module (TEM) [2]. The Peltier thermo-electric effect has two sides, a p-type and n-type semiconductor as shown as in Figure 1. The heat has brought from one side to the other when DC current flows through the device. The Peltier device, creates a voltage when there is a different temperature on each side. Conversely, when a voltage is applied, the temperature difference created. Thus, in principle, the same device can be used for heating as well as cooling purpose by reversing voltage polarities [3].

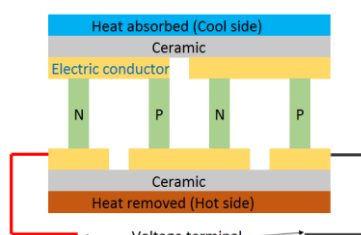


Figure 1 A Peltier device.

In advantages, TEMs are compact, rugged, simple, mechanically not vibrate, scalable, and environmentally

friendly [1-2]. However, thermodynamic efficiencies are below those of alternative technology and limitation in head load for a specified temperature [3].

Temperature control method by using Peltier effect is widely studies in different fields as a cooling application. Thermoelectric coolers (TEC) is the other option for cooling portable equipment due to its robust and reliable in which others cooling device such as air-conditioner and refrigerator are hardly to install [3]. However, a heat sink is needed in Peltier device to minimize conduction resistance [4].

2. A TEMPERATURE-CONTROLLED DEVICE

In this work, a temperature-controlled device by using Peltier effect is proposed and developed. The thermoelectric cooling (TEC) device able to use in certain temperature as required. The temperature is set to 20°C and 40°C for testing and able to use in certain application. The development of temperature controlled device can be divided into three parts which are mechanism system design, software system design and electrical system design. The mechanism system design is focused on mechanical part of the temperature controlled device meanwhile in software design develops programming for controlling temperature and power of Peltier. In electrical system, a control unit is constructed by using temperature sensor, relay module and Peltier as well as Arduino.

Control unit is the main part as shown in Figure 2. The temperature control is used to control the temperature of the system. Temperature sensor, DS18B20 will detect physical environment and convert to electrical signals that sent to the microcontroller and control the temperature.

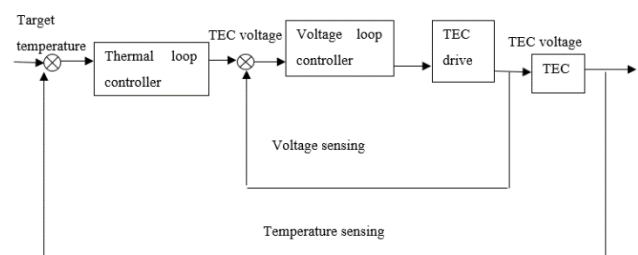


Figure 2 Control block system.

A structure of temperature controlled device is made by polystyrene. The structure of temperature controlled device consists of three parts which are the

main body, the cover box of circuit and the base board. The polystyrene box used to keep water either in cold or hot temperature. Dimension of the box is 22cm x 29cm x 19cm with maximum of 10 litres of water. Figure 3 shows the mechanism of temperature controlled device by using Peltier effect.



Figure 3 A controlled temperature device.

After the complete assembly all parts, performance of temperature-controlled device has been analysed both on cooling and heating process. The measurement for water temperature, current and voltage are obtained by using temperature sensor, clamp meter and multimeter respectively.

3. RESULTS AND DISCUSSION

An observation and analysis of all relevant testing for the development of temperature control device using Peltier effect have been carried out. There are two set points in this work which are cooling process set point and heating process set point with 20°C and 40°C respectively. Two liters of water with a room temperature of 27°C is set for initial condition for both cooling and heating process. Figure 4 shows a graph of time taken for a device to reach set point. The device takes more than 3 hours to achieve the set point.

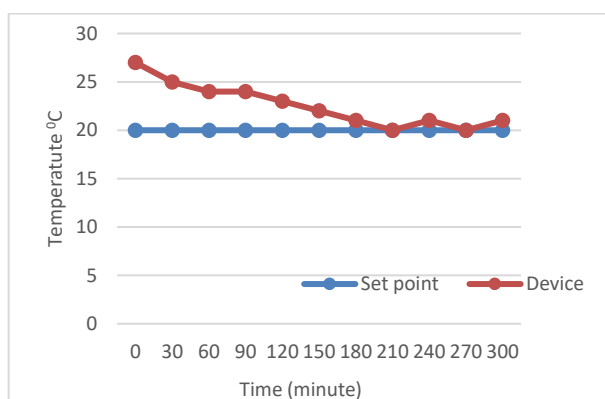


Figure 4 Cooling process.

Figure 5 shows a graph for heating process. It takes 2 hours to achieve set point of 40°C. In comparison, heating process takes longer time to reach set point due to higher temperature differences from room temperature. The device takes 0.0333°C/min to approach the set point in cooling process meanwhile 0.1083°C/min to approach the set point in heating process.

Power consumption for Peltier, fan and Arduino

board are measured to analyze the effect of temperature on a device. Table 1 shows the power consumption in kilowatt-hour (kWh) of these components.

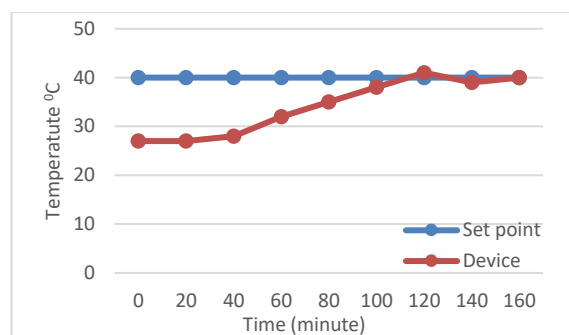


Figure 5 Heating process.

Table 1 Power consumption.

Component	Power (kWh)
Peltier	0.016
Fan	0.0024
Arduino board	0.0025

4. CONCLUSION

As conclusion, the development of temperature controlled device by using Peltier effect is successfully achieved. The device powered by battery and portable. The result has shown that the device able to reach set temperature both in heating and cooling process which is 20°C and 40°C respectively. However, there is overshoot occurs in both process and further study can be done to overcome this problem

ACKNOWLEDGEMENT

The authors would like to thanks Universiti Teknikal Malaysia Melaka (UTeM) for the Short Term Research University Grant No PJP/ 2015/ FTK(23A)/ S01443.

REFERENCES

- [1] J.P. Carmo, L. M. Goncalves and J.H. Correia, "Improved p- and n-type thin-film microstructures for thermoelectricity," in *Electronics Letters*, vol. 45, no. 15, pp. 803-805, 2009.
- [2] M. Hodes, "Optimal design of thermoelectric refrigerators embedded in a thermal resistance network," in *IEEE Transactions on Components, Packaging and Manufacturing Technology*, vol. 2, no. 3, pp. 483-495, 2012.
- [3] R. Sharma, V.K. Sehgal and Nitin, "Peltier effect based solar powered air conditioning system," *2009 International Conference on Computational Intelligence, Modelling and Simulation*, Brno, pp. 288-292, 2009.
- [4] S. Maruyama, A. Komiya, H. Takeda and S. Aiba, "Development of precise-temperature-controlled cooling apparatus for medical application by using peltier effect," *2008 International Conference on BioMedical Engineering and Informatics*, Sanya, pp. 610-614, 2008.

Investigation of Multiple Cooling Coil Effect in Hydronic Radiant Cooling System

A.A.M. Damanhuri^{1,2,*}, A.M.H.S. Lubis^{1,2}, A. Ibrahim^{1,2}, K.A. Kamaruzzaman^{1,2}, M.H. Rosli¹, M.R. Pawanteh¹

¹⁾ Faculty of Engineering Technology, Universiti Teknikal Malaysia Melaka,
Hang Tuah Jaya, 76100 Durian Tunggal, Melaka, Malaysia

²⁾ Centre for Advanced Research on Energy, Universiti Teknikal Malaysia Melaka,
Hang Tuah Jaya, 76100 Durian Tunggal, Melaka, Malaysia

*Corresponding e-mail: amir.abdullah@utem.edu.my

Keywords: Hydronic; thermal comfort; cooling coil

ABSTRACT – Hydronic Radiant Cooling (HRC) is an alternative system that produce cold water as a medium transport. In addition, the system be able to reduce an electrical consumption since the use of compressor is not required. This current study focus on possibility of using Hydronic Radiant Cooling in achieving thermal comfort and humidity. Pump 0.35 kW used to supply 30 litre chilled water to the particular coil. This project successfully reaches optimum temperature and humidity based on Malaysia temperature and relative humidity for thermal comfort that are between 23°C to 26°C and 30% to 60% using triple cooling coil. Design, fabrication and experimental of the project are presented in this paper. The used of HRC achieved 13°C at the coil thus heading to meet thermal comfort temperature.

1. INTRODUCTION

In recent years, system that provide more comfortable thermal environment than conventional all-air system has been created. The system is designed to reduce energy consumption in the line with current modern technology. An alternative system is called Hydronic Radiant Cooling (HRC) [1] which is only using water as the cooling sources. It is becomes one of the significant solutions since it is able to reduce amount electrical consumption in the buildings. In western countries, HRC is usually install inside the ceiling, wall and floor. Unlike the conventional air conditioning system, HRC does not use a vapour compression cycle that consume almost 40% of total energy consumption. Cold water are used to replace refrigerant as a cooling medium which is unlimited source, cheapest and also environmental friendly. The natural cooling provided by HRC is more acceptable range for thermal comfort [2].

In this current study, an air handling unit (AHU) which are used in centralized system will be design, fabricate in prototype and tested the application for alternative cooling in Malaysia. HRC are connected to cooling coil to supply cold water in AHU system. In addition, fan is required to force the conditioned air to a building space. The second important components of an AHU are the cooling elements which are used to allow

cold water flow into the system [3]. So that, the parameter to be considered is the distance between fan and cooling coil, number of row, and oriental of the system design. The temperature and relative humidity must be focus to ensure this application is able to apply in hot climate country such as Malaysia.

2. METHODOLOGY

The first stage of designing the chamber (Figure 1) focused on preparation the key parameter in evaluating the chamber performances. Dimension consideration of chamber which is one of the important approaches before assembly process. The dimension of chamber has been selected to be 1.4m (l) x 0.24 m (w) x 0.255 m (h) based on the fan specifications. The fan flow rate that has been used in the current project is 550 CFM.

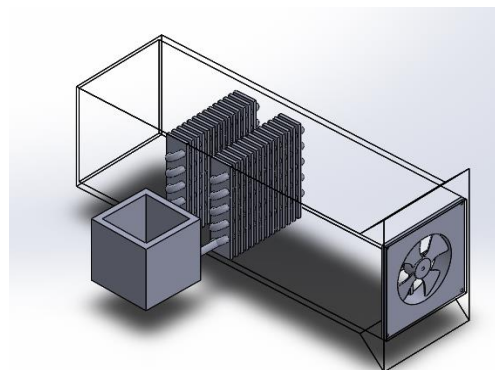


Figure 1 Schematic of chamber.

Three unit of a Proton Waja coil were used in this experiment. The dimension of the cooling coil is 0.24 m (l) x 0.255 m (h) x 0.08 m (w). The cooling coil were located 30 cm from the fan. Pump were used to deliver chilled water through the cooling coil. The specifications of the pump are 240 V, 50 Hz, 0.37 kW and 25 L/min. 30 litre water and 30 kg of ice cube were used to obtain - 5 °C which similar to chilled water supply to conventional air handling unit system. Fluke temperature sensor were used to obtain temperature and humidity data. Tachometer and anemometer also used in monitoring the fan speed and air flow speed.

3. RESULTS AND DISCUSSION

The complete chamber was presented in Figure 2 below. Acrylic thickness 5mm were chosen to be chamber wall, and insulated copper as chilled water medium to spread to the cooling coil.



Figure 2 Chamber experiment set up.

Table 1 Data obtain by using double and triple number of coil.

Qty of coil	Temperature (°C)		Relative Humidity		Velocity (m/s)	
	Inlet	Outlet	Inlet	Outlet	Inlet	Outlet
2	27.6	15.2	67	50.6	3.34	2.1
3	26.1	13.0	64	43.2	3.34	1.9

From Figure 3 and 4 presented, temperature output of double cooling coil is slightly decrease from an ambient temperature to the inlet (before cooling coil). The temperature is rapidly decrease from 27.6°C to 15.2°C. This might be due to the number of cooling coil. So that, the air is repeatedly being cooled in the system and the temperature drop immediately. By referring the case 3 (triple cooling coil), the temperature curve quietly similar with a case 2(double cooling coil). The temperature is suddenly dropped from 26.1°C to 13°C. To achieve the thermal comfort in Malaysia, the required relative humidity is between 30% to 60%. By referring to the graph, relative humidity for double and triple cooling coil has achieved required thermal comfort. In double cooling coil, the RH drop from 67% to 50.6%. Meanwhile by using triple cooling coil the RH drop from 64% to 43.2%.

4. SUMMARY

The experimental conduct in this experiment is to determine the effect of multiple cooling coil used in Air Handling Unit system. Thermal comfort for human used has been achieved by using a HRC as a cooling source. The temperature and relative humidity range is between 23°C to 26°C and 30% to 60%. The lowest temperature based on the result is 13°C by using triple cooling coil. Furthermore, for relative humidity (RH) is 43.2%. In conclude, the HRC system is able to apply in Malaysia as it achieved the required thermal comfort [4].

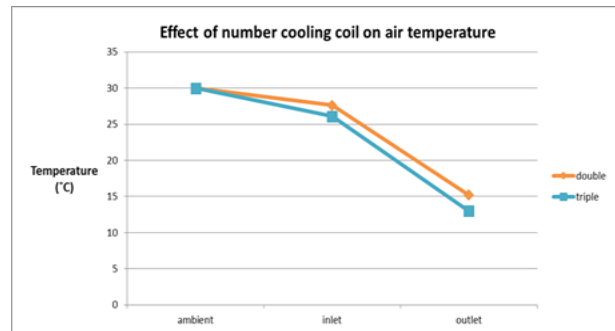


Figure 3 Effect double and triple coil on air temperature.

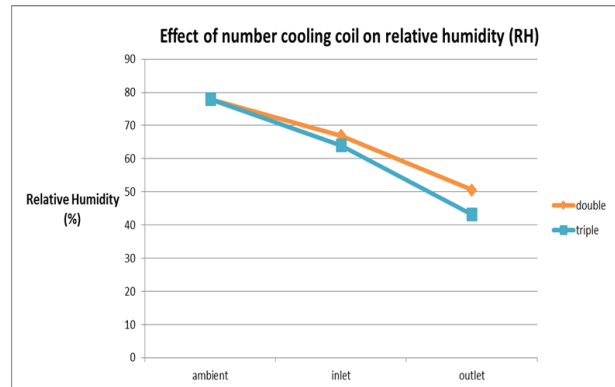


Figure 4 Effect double and triple coil on relative humidity.

ACKNOWLEDGEMENT

The author would like to gratitude and acknowledge Universiti Teknikal Malaysia Melaka for the funding under short term grant PJP/2015/FTK(32A)/S01458.

REFERENCES

- [1] H.E. Feustel, "Hydronic radiant cooling overview and preliminary performance assessment hydronic radiant cooling overview and preliminary performance assessment", *SciTech Connect*, 1993.
- [2] C. Greg, Hydronic systems provide better energy efficiency, http://www.radiantprofessionalsalliance.org/Documents/HIAC/Hydronic_Systems_Provide_Better_Energy_Efficiency-PME.pdf
- [3] G. Wang, & L. Song, "Air handling unit supply air temperature optimal control during economizer cycles," *ASME International Mechanical Engineering Congress and Exposition*, vol. 6, 2012.
- [4] J. Carson, Air handling unit design for high performance building, *International High Performance Buildings Conference Purdue*, 2010
- [5] ASHRAE, Thermal environmental conditions for human occupancy, ANSIASHRAE 2013.

Feasibility study on harvesting wind energy from cooling tower outlet

M.A. Mahasan^{1,2,*}, W.T. Chong¹, J.B. Goh², J. Fairul Azni², A.M. Najib², M.S. Seha²

¹) Department of Mechanical Engineering, Faculty of Engineering, University of Malaya, 50603 Kuala Lumpur, Malaysia

²) Faculty of Manufacturing Engineering, Universiti Teknikal Malaysia Melaka, Hang Tuah Jaya, 76100 Durian Tunggal, Melaka, Malaysia

*Corresponding e-mail: mahasan@utem.edu.my

Keywords: Cooling tower; potential power; wind speed

ABSTRACT – Wind energy is one of the world's most clean renewable energy sources. Due to our country geographic conditions, the natural wind source is not suitable for a wind turbine to be implemented as the average wind speed is between 2 – 3m/s. Due to this limitation, an innovative method needs to be found if we want to venture into wind energy sector. This paper studies the possibility of harvesting wind power from a cooling tower outlet. Three different type cooling tower were used in this investigation. Data shows a promising figure of up to 10m/s wind flow were observed. By calculations, this translates to 4.5kW of potential energy. The amounts of energy calculated were too good to be ignored. Further investigation should be carried out and it should open up new possibilities in energy harvesting.

1. INTRODUCTION

In Malaysia, renewable energy industry is still new. Local experts within the fields are far less than what the country needs. Among the renewable energy sources available in Malaysia are hydropower, solar power, wind power, geothermal and last but not least is tidal power [1].

Based on survey conducted by past researchers, solar and wind energy are the top two type of renewable energy that Malaysians are familiar with as shown in Table 1.

Table 1 Results for renewable energy acceptance in Malaysia [2].

Renewable Energy	Frequency	Percentage %
Solar	472	81
Wind	60	10
Nuclear	24	4
Geothermal	8	1
Tidal	13	2
Don't like	0	0
No opinion	3	1
Total	580	100

For a country where wind blow is highly depending on the monsoons season, the average wind speed throughout the year in Malaysia is around 2.05 m/s [3]. With this wind speed, it is not economically feasible to use a wind turbine as a method to produce

the much-needed electricity as most wind turbine has a cut off speed of 3 – 4 m/s of wind speed [4]. If this technology is to be used, the wind need to be manipulated in order to increase the speed or other type of wind with suitable speed need to be identified. Between these two options, we decided to go for the later.

2. METHODOLOGY

Figure 1 shows the overall steps taken in completing the intended studies conducted. First, an alternative source of wind was selected. One of the suitable sources of unnatural wind is from a cooling tower unit. Table 2 shows all three type of cooling tower unit involved in this study.

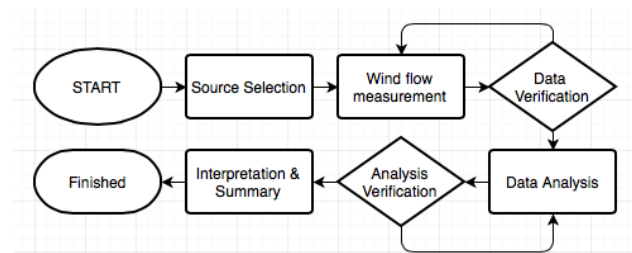





Figure 1 Research methodology.

Table 2 Cooling tower.

Type	Cooling Tower
Type 1 Makes: YORK Size = 840 mm x 1990 mm x 1830 mm Outlet diameter = 760 mm Number of outlet = 2	
Type 2 Makes: Unknown Size = 3830 mm x 4680 mm x 3050 mm Outlet diameter = 2100 mm Number of outlet = 2	
Type 3 Makes: Genius Size = 10020 mm x 4400 mm x 3500 mm Outlet diameter = 2000mm Number of outlet = 4	

Then, the wind speed from each cooling tower outlet were measured and recorded using a wind flow meter. Five readings were taken for each cooling tower unit. Each reading is an average value taken from three different locations, which are the inner ring, middle ring and outer ring as shown in Figure 2.

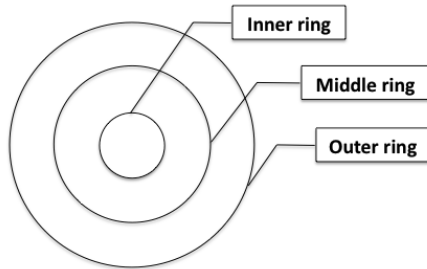


Figure 2 Top cooling tower zone.

Recorded data were analyzed and potential energy from each type of cooling tower was calculated.

$$P = \frac{1}{2} \rho A V^3 \quad [5]$$

Where,

P = power

ρ = air density

A = swept area of blades ($A = \pi r^2$)

V = wind velocity

3. RESULTS AND DISCUSSION

Based on the data gathered in Table 3, all three cooling towers produce wind speed of more than 4m/s and this speed meet the requirement for a wind turbine to be in operation. Type 2 and Type 3 cooling tower show the most promising result as the wind speed recorded is above 8 m/s.

Table 3 Wind speed

	Type 1	Type 2	Type 3
1 st reading	4.90	10.10	8.30
2 nd reading	4.80	10.20	8.35
3 rd reading	4.70	10.30	8.32
4 th reading	4.80	10.20	8.3
5 th reading	4.80	10.10	8.32
Mean	4.80	10.18	8.32
Standard deviation	0.07	0.08	0.02

The data also shows that the standard deviations for all types of cooling tower are 0.07, 0.08 and 0.02 respectively. This shows the output wind from the cooling tower is really stable and it is constant throughout its operating time.

In renewable energy field, constant source is highly valuable and required. This will help the system to generate a much more stable output thus stabilizing the overall system performance.

Table 4 Potential power.

Type	Calculation	Potential Power (Watt)
1	$\left[\frac{1}{2} (1.23) (\pi \times 0.38^2) (4.80^3) \right] \times 2$	61.71
2	$\left[\frac{1}{2} (1.23) (\pi \times 1.05^2) (10.18^3) \right] \times 2$	4494.45
3	$\left[\frac{1}{2} (1.23) (\pi \times 1.00^2) (8.32^3) \right] \times 4$	4450.97

Table 4 shows the potential power for each of the turbine in the investigated cooling tower. For type 1 cooling tower, the potential energy is not so high even though the wind velocity is more than 4 m/s. This is due to the small size of the unit outlet thus resulting a low value of swept area. On the other hand, the other types of cooling tower have more substantial potential power.

4. SUMMARY

From the investigation carried out, the potential energy from the cooling tower outlet is too good to be ignored. Depending on the size of cooling tower itself, the wind blows is up to 10 m/s. This translates into kW of free electrical energy with zero pollution. Harvesting wind energy from this type of source will create a new trend in energy harvesting as Malaysia uses a lot of cooling tower.

Even though it is possible, effects of such system to the cooling tower performance are not known and not covered in this investigation. Further investigation on the cooling tower performance after implementing such system can be investigate further before it is deemed suitable to be used.

REFERENCES

- [1] A.Y. Azman, A.A. Rahman, N.A. Bakar, F. Hanaffi and A. Khamis, "Study of renewable energy potential in Malaysia," *Clean Energy and Technology (CET)*, 2011 IEEE First Conference on, Kuala Lumpur, pp. 170-176, 2011.
- [2] A.W.A. Al-Fatlawi, R. Saidur and N.A. Rahim, "Researching social acceptability of renewable-energy technology in Malaysia," *Clean Energy and Technology (CEAT)* 2014, 3rd IET International Conference on, Kuching, pp. 1-5, 2014.
- [3] A. Belhamadia, M. Mansor and M.A. Younis, "Assessment of wind and solar energy potentials in Malaysia," *Clean Energy and Technology (CEAT)*, 2013 IEEE Conference on, Lankgwawi, pp. 152-157, 2013.
- [4] T. Khatib and A. Mohamed, "A feasibility study for electricity generation using wind power systems in the Malaysian Borneo," *Power and Energy (PECon)*, 2012 IEEE International Conference on, Kota Kinabalu, pp. 594-598, 2012.
- [5] S. Mathew, *Wind energy: fundamentals, resource analysis and economics* (vol. 1), Heidelberg: Springer, 2006.

Energy audit in Malaysia public hospital

M.I.M. Hafiz*, M.F. Sulaima

Centre for Advanced Research on Energy, Universiti Teknikal Malaysia Melaka,
Hang Tuah Jaya, 76100 Durian Tunggal, Melaka, Malaysia

*Corresponding e-mail: mohamedhafiz@utem.edu.my

Keywords: Energy audit, public hospital

ABSTRACT – Malaysia has pledge to reduce its carbon emission intensity in 2030 by 45% compare to carbon emission intensity in 2005. Energy consumption from government hospital is one of the contributor to the carbon emission. Therefore, implementation of energy audit is essential to define the energy losses and create the opportunity to get saving. The result indicates that annual energy consumption is 3,113,330kWh and six energy conservation measures has been identified to reduce the energy consumption. The payback period for the measures implementation is 2.77 years.

1. INTRODUCTION

Malaysia has pledge to reduce its carbon emission intensity of Gross Domestic Products (GDP) by 45% by 2030 relative to the emission intensity of GDP in 2005 [1]. In achieving this target, 11th Malaysia Plan has set 10 strategic thrusts which include the pursuing green growth for sustainability and resilience which has become the 6th strategic thrust. Under this thrust, adopting the sustainable production and consumption has been put as one of the key focus area which embedded the enhancing demand side management of energy consumption [2].

Recently, a new agreement between the has been made between government and concessionaire company to implement Energy Performance Contracting (EPC). The objective is to ensure the asset is properly maintained and reduce the energy consumption in the respective hospital. One of the component for embarking the EPC is conducting the energy audit.

Energy audit has been conducted at Hospital Port Dickson (HPD), Negeri Sembilan. HPD is a nucleus hospital which has 110 beds with Bed Occupancy Rate (BOR) at 85% in 2014. The building main energy supply are in the form of electricity from TNB (100%).

2. METHODOLOGY

The important steps involve in conducting the energy audit as follows:

1. Desktop data collection;
2. Review of building operation and utilization factor;
3. On site measurement; and
4. Development of energy conservation measures.

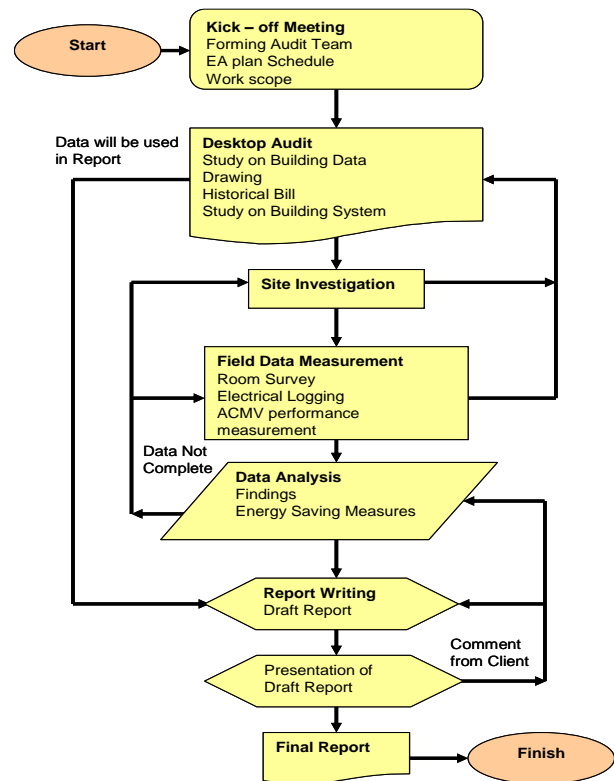


Figure 1 Energy audit flow chart.

Figure 1 shows the energy audit flow chart at HPD. The onsite measurement has been conducted for two weeks at HPD where the duration from kick off meeting until final report submitted is two months. The process was strictly follow from the guidebook published by Energy Commission (EC) [3].

3. RESULTS AND DISCUSSION

3.1 Historical bill analysis

The annual energy consumption at HPD is 3,113,330kWh which is equivalent to RM1,565,880. Figure 2 shows the monthly energy consumption at HPD. Based on the figure, the average energy consumption is 259,444 kWh while the highest energy consumption is in December 2015. On the other hand, the lowest energy consumption is in February 2015. This is related with the lowest cooling degree days (CDD) and number of outpatients at HPD.

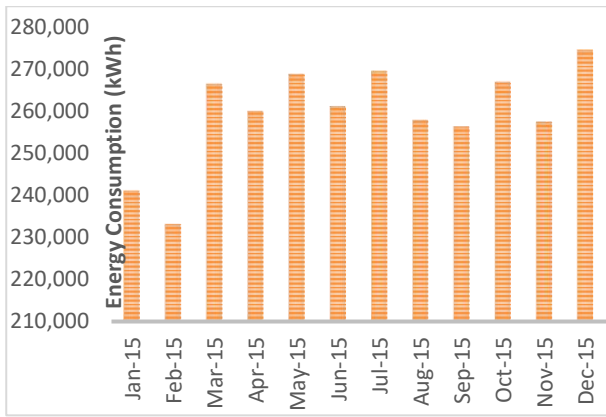


Figure 2 Monthly energy consumption at HPD.

Further analysis was performed to determine the correlation between the energy consumption and the impact independent variables, namely number of outpatients and CDD. Single linear regression analysis was performed and the results shows that the coefficient value, R^2 for CDD and number of outpatients is 0.2504 and 0.1191 respectively. These values indicate that single variable correlation is less significant.

Therefore, a multiple linear regression was performed by combining both independent variables. The result shows that the correlation value is 0.77 with intercept value of 47,929kWh. The value indicates that by combining both independent variables, it is significant with energy consumption at HPD.

3.2 Power load apportioning

Load apportioning analysis was performed to identify the highest power consumption. Figure 3 shows that highest power consumption is from air conditioning unit comprising the air handling unit, chilled water pump and suction water pump. Next, is the lighting followed by plug load, compressed air system, boiler, and hot water system. Therefore, the energy conservation measures should have focus on air conditioning unit to gain significant reduction of energy consumption.

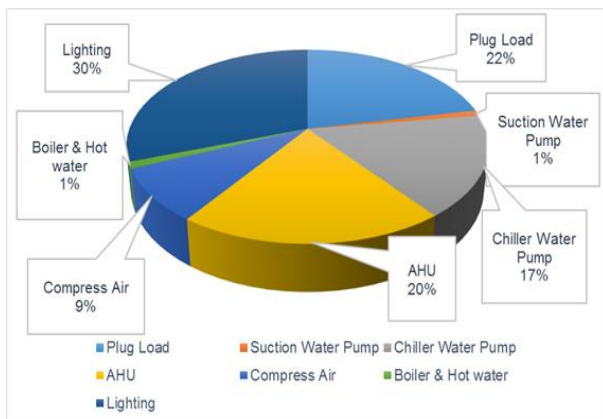


Figure 3 Power load apportioning at HPD.

3.3 Energy conservation measures (ECMs)

The development of ECMs is based on the technical and financial constraint found at HPD. The financial is evaluated by the duration of payback period. Table 1 shows the ECM suggests for HPD.

Table 1 ECMs suggestion for HPD.

Energy Conservation Measures	Potential Saving		Investment (RM)	Payback Period (year)
	Energy (kWh)/Year	Cost (RM)/Year		
Improving SEMS	93,400	47,526	15,000	0.32
Control & Monitoring of base load	96,000	48,849	10,000	0.2
Re-lamping of 950 units T8F to T8 LED	106,552	54,220	182,023	3.36
Retrofit for CFL 13W to LED 8W	2,593	1,305	1,850	1.42
Retrofit of the EE Air-conditioning (Split Unit) Tariff G	311,333	158,454	1,437,500	9
Transform for Street Lighting		5,829	13,500	2.32
Total	609,878	310,353	1,659,873	2.77

Overall, 6 ECMs were suggest for HPD. Total investment requires to implement all the 6 ECMs is RM1.7 million with payback period is less than 3 years. Total energy and cost saving is 609,877 kWh/year and RM 310,353 respectively.

4. CONCLUSION

In conclusion, total potential energy saving for HPD if all the ECMs implement is approximately 19% while for the cost reduction is 19.8% congruently.

ACKNOWLEDGEMENT

The project would like to acknowledge the Ministry of Health, HPD, Medivest Sdn. Bhd., Taiace Engineering Sdn. Bhd. and Universiti Teknikal Malaysia Melaka for the financial and technical assistant for this project.

REFERENCES

- [1] New Straits Times Onlines, "Malaysia is on track to hit carbon emission reduction target: PM Najib," Media Prima Berhad, 19 03 2016. [Online]. Available: <http://www.nst.com.my/news/2016/03/133719/malaysia-track-hit-carbon-emission-reduction-target-pm-najib>. [Accessed 31 12 2016].
- [2] Malaysia Economic Planning Unit, "11th Malaysia Plan," 21 05 2015. [Online]. Available: <http://www.micci.com/downloads/11MP.pdf>. [Accessed 31 12 2016].
- [3] Malaysia Energy Commission , Electrical Energy Audit Guidelines for Building, Putrajaya: Malaysia Energy Commission, 2016.

Briquetting of water hyacinth: Thermal pretreatment study

N.M.M. Mitani^{1,*}, M.S. Hafiz Rajemi²

¹Faculty of Engineering Technology, Universiti Teknikal Malaysia Melaka, Hang Tuah Jaya, 76100 Durian Tunggal, Melaka, Malaysia

²Faculty of Mechanical Engineering, Universiti Teknikal Malaysia Melaka, Hang Tuah Jaya, 76100 Durian Tunggal, Melaka, Malaysia

*Corresponding e-mail: nona.merry@utem.edu.my

Keywords: Water hyacinth; thermal pretreatment; briquette

ABSTRACT – Water hyacinth is an aquatic plant that causes the problem to the environment especially in the river. The purpose of current study is producing the briquette from water hyacinth with main focus on drying effect of pretreatment the water hyacinth. Six steps consist in briquetting of water hyacinth as a feedstock through drying (natural drying and oven drying at 100 °C), crushing, milling, carbonization at 350 °C and densification by hydraulic press. Proximate analysis revealed the lowest moisture content, volatile matter and fixed carbon was found in briquette from oven drying [C(O)] with percentage 4.67, 34.0 and 9.00 % respectively. Lowest ash content produced by non-carbonized briquette from oven drying of feedstock [NC(O)] which was 19.00 %. Carbonization briquette from natural drying of feedstock [C(ND)] has the highest calorific value.

1. INTRODUCTION

Water hyacinth is a pest that lives on the water such as river and lake. It does not only destroy the ecosystem of water, but also seriously caused depletion water bodies of oxygen, loss of water and increasing breeding ground for mosquitoes. Instead of that, the faster growing of water hyacinth makes the dense mat on the surface of the water along river or lake [1].

The components presence in water hyacinth namely cellulose, hemicellulose, lignin and ash make it possible to process as a candidate for renewable energy in form of briquette [2].

Densification of biomass become briquette or pellet is well known technique to reduce the volume and increase the calorific value of the biomass. The common biomass such as wood sawdust [3], sugarcane and coconut shell [4], soda weed [5], durian peel [6] and reed [7] were applied as raw material for briquette to substitute the coal. This present research reported potential biofuel from water hyacinth in a briquette form and in particular observed the effect of drying process as an important step for briquetting.

2. METHODOLOGY

Preparation of water hyacinth samples. The raw materials of water hyacinth were from rivers around Malacca area. Prior to use, the samples are cleaned from the mud at their roots and free from contaminants. The

cleaned water hyacinth was cut into pieces and dried with two conditions that are drying by using air-circulating oven at 100 °C for 24 hours and natural drying. Natural drying means that sample was dried under sunlight for three days in open space. In order to observe the lost weight, the water hyacinth sample was weighed before and after drying.

The next process after drying was crushing to reduce the size of samples. Crushed samples are required for milling. The crushed samples were milled by a centrifugal milling machine (Retsch ZM 200) with 0.75 mm of mesh size. Furthermore, the milled samples were carbonized in the electrical furnace at 350 °C for 40 min. with heating rate of 10 °C/min.

Densification of non-carbonized and carbonized samples was conducted with hydraulic press (Hsin-Chi Machinery HL 200) equipped by cylinder mold. It has inner diameter of 35 mm and its thickness is 10 mm. This process was conducted under 50 MPa pressing load of hydraulic press. The code of briquettes is provided in Table 1.

Table 1 Four types of water hyacinth briquette

Water hyacinth briquettes	Codes
Non-carbonized briquette from natural drying of feedstock	[NC(ND)]
Non-carbonized briquette from oven drying of feedstock	[NC(O)]
Carbonized briquette from natural drying of feedstock	[C(ND)]
Carbonized briquette from oven drying of feedstock	[C(O)]

Characterization of water hyacinth briquette. A Proximate analysis of the briquette was performed to quantify the moisture content, volatile matter, ash content and fixed carbon. These analyses were carried out according to the American Society for Testing Materials (ASTM) D 3173-03, ASTM D 3175-02 and ASTM D 3174-02 standards [8]. The heating value of the briquette was determined experimentally by using bomb calorimeter IKA C200. To evaluate the strength of briquette, the compressive test was conducted by Universal Testing Machine Instron 5583.

3. RESULTS AND DISCUSSION

Proximate analysis is carried out to characterize the briquette products. The analysis involved moisture content, volatile matter, ash content and fixed carbon as shown in Figure 1.

Moisture content is the important aspect for briquetting water hyacinth. The higher value of moisture content will lower the calorific value of briquette. From Fig. 1, both of carbonization briquettes have the lower percentage of moisture content compare to the non-carbonized briquettes.

Volatile matter has a role in producing smoke during combustion of briquette. Volatile matter reveals gaseous content such as hydrocarbon, methane and incombustible gaseous. The non-carbonization briquettes did not undergo burning process, so that produced high percentage of volatile matter. Meanwhile, the carbonized briquettes have lower content of volatile matter than non-carbonized briquettes. The results also show that drying process did not bring the significant effect on volatile matter.

The remaining residue left after the combustion is known as ash content. The presence of ash content in both carbonization briquettes is higher than non-carbonization briquette. Drying method has no strong effect on percentage of ash content.

Fixed carbon is considered as a carbon friction in briquette along with moisture content, volatile matter and ash content. The high percentage of fixed carbon from carbonized briquette shown that carbonization will raise the carbon fraction in briquette. Furthermore, the all drying methods show similar results in fixed carbon.

As a requirement for solid biofuel, calorific value test was carried out for all briquettes. The carbonized briquettes for both drying methods have higher value than non-carbonized briquettes as shown in Fig. 2 (about 3,500 Cal/g).

In order to ensure the quality of briquette, compressive test was performed for storage and logistic purposes. Non carbonized briquette from natural drying has the highest compressive strength as shown in Table 1.

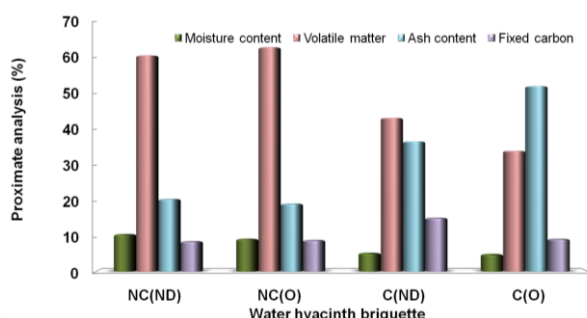


Figure 1 Proximate analysis of water hyacinth briquettes.

4. SUMMARY

The four types of briquette succeed produced from water hyacinth. Both thermal pretreatment through natural and oven drying has less difference in proximate analysis and calorific value of briquette. Natural drying

can become alternative for save energy in processing water hyacinth to briquette.

Furthermore, proximate analysis is important due to impact to the calorific value of briquette. In order to achieve the good quality of briquette, several characters are required: a) The lower moisture content to produce higher calorific value; b) Reducing the smoke release during combustion from volatile matter content; c) Lower ash content due to high ash content is less desirable for energy production of solid biofuel.

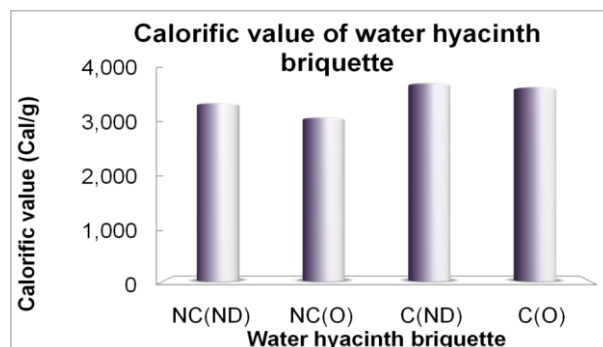


Figure 2 Calorific value of water hyacinth briquettes.

Table 2 Compressive tests of water hyacinth briquettes.

Briquettes	Compressive strength (MPa)
NC(ND)	103.186
NC(O)	86.217
C(ND)	77.357
C(O)	58.200

REFERENCES

- [1] F.O. Agunbiade, L. Bamidele, O. Owolabi, and K.O., Adebawale, Phytoremediation potential of *Eichornia Crassipes* in metal contaminated coastal water," *Bioresource Technology*, vol. 100, 4521-4526, 2009.
- [2] A. Bhattacharya and P. Kumar, "Water hyacinth as a potential biofuel crop," *Electronic Journal of Environmental, Agriculture and Food Chemistry*, vol. 9, 112-122, 2010.
- [3] L. Kong, SH. Tian, C. He, C. Du, YT. Tu, and Y. Xiong, "Effect of waste wrapping paper fiber as a "solid bridge" on physical characteristics of biomass pellets made from wood sawdust," *Applied Energy*, vol. 98, pp 33-39, 2012.
- [4] N.M.M., Mitan and M.N.S.A., Razimi, "Potential co-processing of coconut shell and sugarcane residue as a solid biofuel". *Proceedings of Mechanical Engineering Research Day 2016*, Centre for Advanced Research on Energy, Universiti Teknikal Malaysia Melaka, Malaysia, 2016, pp. 83-84
- [5] H. Yumak, T. Ucar, and N. Seyidbekiroglu, "Briquetting soda weed (*Salsola tragus*) to be used as a rural fuel source," *Biomass and Bioenergy*, vol. 34, pp. 630-636, 2010.
- [6] N.M.M., Mitan, A. H., Azmi, N.F.M. Nor, and S.M. Se, "Binder application in durian peels

- briquette as a solid biofuel", *Applied Mechanics and Materials*, vol. 761, pp. 494-498, 2015.
- [7] C. Coşereanu, G. Budău, D. Lica, A. Lunguleasa, and CR Gheorghiu, "Technological potential of reed as a biomass for briquetting," *Environmental Engineering and Management Journal*, vol. 10, pp. 1127-1132, 2011.
- [8] American Society for Testing and Materials, Annual Book of ASTM Standards, Designation D 3173-03, D 3174-02 and D 3175-02, 2002.

A study on joint probability density function for wind data in Mersing, Malaysia

N. Sanusi^{1,2,*}, A. Zaharim², S. Mat²

¹⁾ Faculty of Mechanical Engineering, Universiti Teknikal Malaysia Melaka, Hang Tuah Jaya, 76100 Durian Tunggal, Melaka, Malaysia

²⁾ Solar Energy Research Institute, Universiti Kebangsaan Malaysia, 43600 UKM Bangi, Selangor, Malaysia

*Corresponding e-mail: nortazi@utem.edu.my

Keywords: Joint distribution; gamma; finite mixture of von Mises

ABSTRACT – Exact information on wind power density in an area is a vital in studying the potential of generating wind energy. This research is conducted purposely to study the joint distribution of wind speed and direction and its effect in wind power density. The Monte Carlo is selected as a method in solving the integration problem. The analysis reveals that the joint distribution used for estimating mean power density is fit in describing the variation in the data and gives a consistent result for the seven years data of Mersing, Malaysia.

1. INTRODUCTION

The previous study [1] on wind data of Mersing, Malaysia was focusing on the wind speed and wind direction separately. Then, the estimated mean wind power was revealed.

This research is purposely designed to estimate the mean wind power of a joint distribution of wind speed and wind direction. Studies of the joint distribution of wind speed and wind direction have been done abroad such as [2], [3]. But, in the case of Malaysia wind data, there is no such research has been done so far. Therefore, it is hope that this study will initiate a broad spectrum of studying the joint distribution of wind data in Malaysia.

2. METHODOLOGY

The joint distribution discuss in this research is basically a bivariate model of wind speed and wind direction that represents Mersing wind data. Parameters for both distribution is first to be estimated by using the Expectation Maximization (EM) method.

Four distributions tested for wind speed which are Weibull, Gamma, inverse Gamma and Burr. While, for the wind direction, the finite mixture of von Mises distribution is selected as it provides a very flexible model for wind direction and it capable to represent several modes or prevailing wind directions data.

Equation (1) and (2) show probability distribution function (pdf) for Gamma and finite mixture von Mises, respectively.

$$f(x) = \frac{1}{\Gamma(\alpha)\beta^\alpha} x^{\alpha-1} \exp\left(-\frac{x}{\beta}\right) \quad (1)$$

$$f_\theta(\theta) = \sum_{j=1}^H \frac{\omega_j}{2\pi I_0(\kappa_j)} \exp\left[\kappa_j \cos(\theta - \mu_j)\right] \quad (2)$$

For $0 \leq \theta < 2\pi$

The two pdf is then being combine in a joint distribution function based on the method that proposed by [4] that has been used widely in the angular-linear distribution analysis and application. The general pdf is shown in Equation (3)

$$f_{v,\theta}(v, \theta) = 2\pi g(\xi) f_v(v) f_\theta(\theta) \quad (3)$$

For $0 \leq \theta < 2\pi$; $-\infty < v < \infty$

The best joint distribution of wind speed and wind direction is selected, based on the goodness-of-fit test. The R^2 coefficient value is one of the indicator in the goodness-of-fit test. Formula for R^2 correlation coefficient as in Equation (4):

$$R^2 = \frac{\sum_{i=1}^n (\hat{F}_i - \bar{F})^2}{\sum_{i=1}^n (\hat{F}_i - \bar{F})^2 + \sum_{i=1}^n (F_i - \bar{F})^2} \quad (4)$$

For;

F_i is a cumulative data function

\hat{F}_i is the estimate cumulative distribution function

$$\bar{F} = \frac{\sum_{i=1}^n \hat{F}_i}{n}$$

The selected joint distribution of wind speed and wind direction (which is Gamma and finite mixture von Mises) is then uses for estimating the mean of wind power density by using Equation (5)

$$\bar{P} = \iint_0^{\frac{1}{2}} \frac{1}{2} \rho V^3 f_{v,\theta}(v, \theta) dv d\theta \quad (5)$$

For Malaysia case, the value of air density, $\rho = 1.16\text{kg/m}^3$ [5]. The double integration in Equation (5) is solved by using the Monte Carlo method. This method solves a problem by generating suitable random numbers and use iteration techniques for obtaining numerical solutions to the integration problem. The value of mean wind power density is in W/m^2 . This value is representing the wind power available per unit area. All the analysis in this study is resolved by using MATLAB R2014a.

3. RESULTS AND DISCUSSION

Among all four proposed combination of wind speed and wind direction distribution being studied in this research, the joint distribution of Gamma and finite mixture of von Mises is the best distribution that explained Mersing data very well. Based on R^2 coefficient which is 0.99861, it indicates that 99.861 percent of the variation in the data can be explained by the joint distribution. Table 1 shows the value of R^2 coefficient for all four proposed joint distributions.

Table 1 R^2 coefficient value for each proposed joint distribution.

Proposed joint distribution	R^2 value
Weibull-finite mvM	0.92543
Gamma- finite mvM	0.99861
Inv Gamma- finite mvM	0.95762
Burr - finite mvM	0.94578

Table 2 shows the mean wind power density (W/m^2) of Mersing data for the year of 2007 to 2013. This result is estimated using the joint distribution of Gamma and finite mixture von Mises. The estimated value of mean wind power density (W/m^2) is varies between 15.60031 to 22.16106 W/m^2 and gives a mean of 16.52373 W/m^2 and standard deviation of 2.10868. It shows that the estimated values for these seven years' data are consider consistent with not much variation. The graph presentation of mean wind power density (W/m^2) for Mersing is shown in Figure 1.

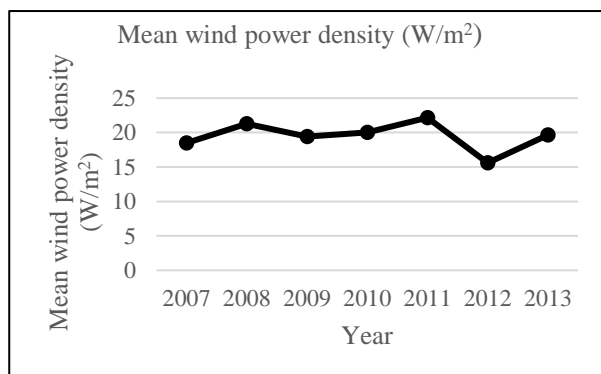


Figure 1 Mean power density (W/m^2).

Table 2 Mean wind power density (W/m^2).

Year	Mean wind power density (W/m^2)
2007	18.51145
2008	21.2624
2009	19.43737
2010	20.02928
2011	22.16106
2012	15.60031
2013	19.66427

4. CONCLUSION

This paper reveals an initial study on joint distribution application for wind data in Malaysia. The joint distribution of Gamma and finite mixture of von Mises for Mersing data is selected as the best joint distribution for representing Mersing data. The value of R^2 coefficient indicates that 99.861 percent of the variation in the data of Mersing can be explained by the selected joint distribution. The complexity of the joint distribution is solved by using the Monte Carlo integration method. The result of the wind power density is significant with the first class of wind power density categories ($<100 \text{ W/m}^2$ and wind speed $<4.4 \text{ m/s}$). Although the value is considering low, but with some innovative actions such as the use of hybrid system of wind and solar, or with a small but highly sensitive wind turbine may lead to wind power generation in Mersing.

REFERENCES

- [1] N. Sanusi, A. Zaharim, and S. Mat, "Wind energy potential: a case study of Mersing, Malaysia," *ARPJ. Eng. Appl. Sci.*, vol. 11, no. 12, pp. 7712–7716, 2016.
- [2] J. A. Carta, P. Ramírez, and C. Bueno, "A joint probability density function of wind speed and direction for wind energy analysis," *Energy Convers. Manag.*, vol. 49, no. 6, pp. 1309–1320, Jun. 2008.
- [3] T. H. Soukissian and F. E. Karathanasi, "On the selection of bivariate parametric models for wind data," *Appl. Energy*, vol. 188, pp. 280–304, 2017.
- [4] Johnson R.E and W. T.E, "Some angular-linear distributions and related regression models," *J. Am. Stat. Assoc.*, vol. 73, p. 363, 1978.
- [5] K. Sopian, "The wind energy potential of Malaysia," *Renew. Energy*, vol. 6, no. 8, pp. 4–6, 1995.

High efficiency and high sensitivity DTMOS differential-drive rectifier for energy harvesting application

A.N.F. Asli, Y.C. Wong*

Micro and Nano Electronic (MINE) Research Group, Centre for Telecommunication Research & Information
Faculty of Electronic Engineering and Computer Engineering, Universiti Teknikal Malaysia Melaka,
Hang Tuah Jaya, 76100 Durian Tunggal, Melaka, Malaysia

*Corresponding e-mail: ycwong@utem.edu.my

Keywords: DTMOS; differential-drive rectifier (DDR); power conversion efficiency (PCE)

ABSTRACT – This paper discusses the efficiency (PCE) of 0.18 μ m CMOS dynamic threshold voltage (DTMOS) differential-drive rectifier (DDR) for energy harvesting application which can be improved by the use of decoupling capacitor between the cross-connected drain-and-gate transistors at the rectifier. The proposed design achieves 80.6% PCE at input power, $P_{in} = -23.5$ dBm and produces an output of 503.1mV at input frequency, 900MHz and $P_{in(ampitude)} = -12$ dBm. The proposed design enables the rectifier operates in less than 3 times input RF power compared to conventional DTMOS DDR.

1. INTRODUCTION

RF energy harvesting becomes topic of interest recently due to the constant energy sources provided by RF devices. The performance of energy harvesting depends on the efficiency of rectifier. Low threshold voltage, V_{th} and leakage current are the factors that measure the rectifier efficiency. DDR is known for its ability to provide small V_{th} and leakage current simultaneously. However, due to the direct current flows across the parasitic diode in diode-connected MOSFET, large reverse current is flows through the transistor during reverse bias makes the performance of DDR not optimum. DTMOS transistor is introduced where the body is tied to the gate instead to the source terminal. This allows the V_{th} to be controlled dynamically by the gate of transistor thus reducing leakage current and achieving high drain current than that of conventional MOSFET architecture [2]. DTMOS DDR is then introduced to enhance the performance of the rectifier.

All transistors of the rectifier should operate in subthreshold region in order for the device to work at very low input power [4]. To increase the efficiency at low input power, a decoupling capacitor is added into the rectifier which will be discussed in the following section.

The paper is organized as follows: Section 2 discusses the method of proposed design to achieve high efficiency at low power. Section 3 discusses the result of the rectifier followed by conclusion in Section 4.

2. METHODOLOGY

Figure 1(a) shows the conventional DTMOS DDR. Differential input RF signal is applied across the two nodes, V_x and V_y . The gate-to-source voltage, V_{gs} of the

transistors is driven by the voltage applied at node V_x and V_y . The transistors will turn-on when V_x reach the V_{th} . The positive voltage applied at the gate of M_{n2} causing the V_{th} of the device to reduces effectively. During this cycle, M_{n1} and M_{p2} will operate in subthreshold region.

Figure 1(b) shows the DTMOS DDR with a grounded capacitor is applied between the cross-connected drain-and-gate transistors. As discussed earlier, when input signal from the source arrives at V_x , the signal will be directly transferred to its cross-connected gate. All the data of the signal includes the noise is transferred to the gate. By applying decoupling capacitor, the noise coming from input rectifier will be shunted into the capacitor before the input signal is injected into the gate V_x thus increasing its efficiency.

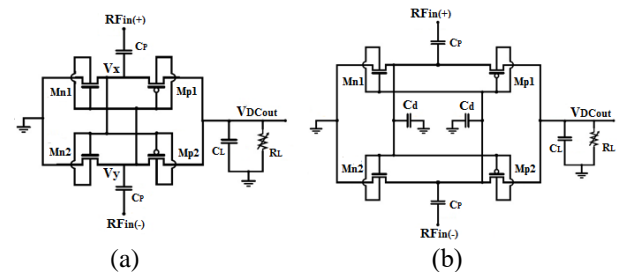


Figure 1 (a) Conventional and (b) proposed DDR.

3. RESULTS AND DISCUSSIONS

The DDR is simulated using Silterra 0.18 μ m CMOS process technology. The effects of the size of decoupling capacitor, C_d and load resistor, R_L to the behavior of the circuit have been investigated. A matching network is applied between the 50 Ω input and the rectifier to reduce the power loss during energy harvesting.

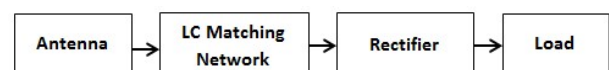


Figure 2 DDR testbench circuit.

At the same parameters as the proposed design, conventional DTMOS DDR achieves 78.62% PCE at $P_{in} = -7.5$ dBm and produces a 453.2mV output voltage. As shown in Figure 3, the proposed design achieves significant better PCE at low input power compared to conventional DTMOS DDR. The peak of the PCE has

now shifted from P_{in} of -7.5dbm to -23.5dbm. The noise coming from the input rectifier is shunted by decoupling capacitor before the signal is injected into the desired gate. This reduces the power loss thus increasing the efficiency of the rectifier.

Figure 4 shows the effects of the C_d to the PCE of the proposed DDR. The PCE slight decreases with the increasing of the capacitor C_d size. This is due to the higher parasitic resistance and inductance in the capacitor, disturbing the performance of the rectifier.

In Figure 5, it is shown that as the R_L increases, the power efficiency at low input power also increases. Higher load produces smaller load current at the output thus causing the output voltage to increase and increasing the efficiency. The rectifier targeting small output current achieves the peak of PCE of 78.66% at P_{in} of -33dB. By drawing more current from the rectifier, the peak PCE has shifted to the right as shown in Figure 5. Note that the transistor size for the result obtained in Figure 5 has been optimized and is extracted in Table 3.

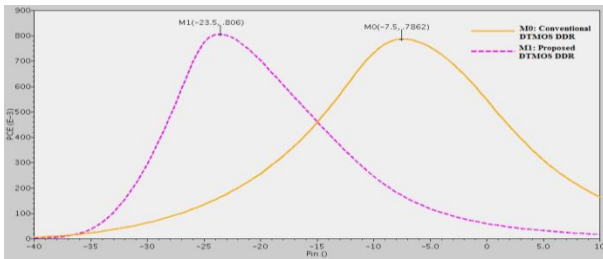


Figure 3 PCE (%) vs input power, pin (dBm) of conventional and proposed DDR at $R_L = 50K\Omega$.

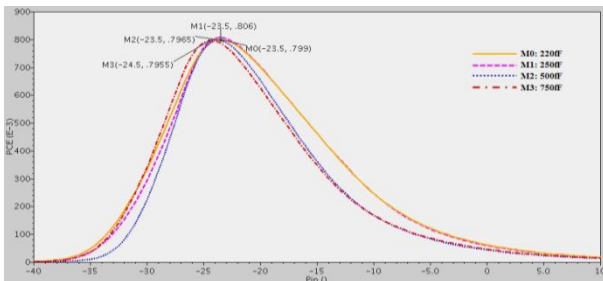


Figure 4. Proposed DDR: PCE (%) vs pin (dBm) for various C_d values at $R_L = 50K\Omega$.

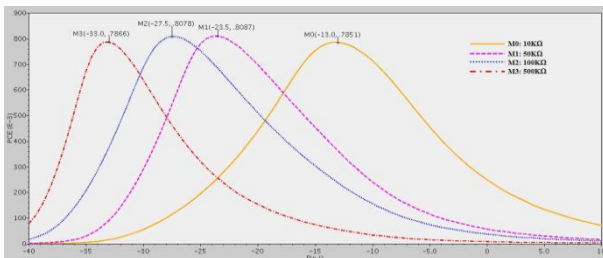


Figure 5 Proposed DDR: PCE (%) vs pin (dBm) for various R_L .

Table 1 Summary of circuit parameters values.

Properties	Conv. DTMOS	Proposed DTMOS
Freq (MHz)	900	900
P_{in} (amplitude) (dBm)	-12	-12
W/L _N (μm/nm)	14/180	14/180
W/L _P (μm/nm)	28/180	28/180
C_P (pF)	5	5
C_d (fF)	-	250
C_L (pF)	7.5	7.5
R_L (KΩ)	50	50

Table 2 Conventional vs. proposed DTMOS DDR.

Simulation Result	Conv. DDR	Prop. DDR
PCE (%) @ P_{in} (dBm)	78.62 @ -7.5	80.60 @ -23.5
V_{out} (mV)	453.2	503.1

Table 3 Optimized transistor size for various R_L values.

Properties	R_L (KΩ)			
	10	50	100	500
W/L _N (μm/nm)	16/180	16/180	16/180	16/180
W/L _P (μm/nm)	32/180	24/180	16/180	16/180

Table 4 Performance benchmarking.

Rectifier Topology	[6]	[3]	[1]	This Work
Year	2009	2015	2016	2017
Tech. (μm)	0.18	0.18	0.18	0.18
Freq. (MHz)	953	433	953	900
W/L _N (μm/nm)	3.6/180	10/180	83.62/180	14/180
W/L _P (μm/nm)	18/180	10/180	472/180	28/180
C_L (pF)/ R_L (kΩ)	1.13//10	10//100	1.13//10	7.5//50
PCE (%) @	75.3@	69.9@	83.35@	80.8@
P_{in} (dBm)	-12.5	-27.4	-16.37	-23.5
V_{out} (mV) @	658@	356.8@	447@0.6	516@
V_{in} (V)	0.92	0.5		0.2754

4. CONCLUSION

This paper presents an enhanced DTMOS DDR that achieves high efficiency at very low input power. The proposed design achieves 80.6% PCE at $P_{in} = -23.5$ dBm and produces an output voltage of $V_{out} = 503.1$ mV at amplitude $P_{in} = -12$ dBm. The sensitivity of the proposed DTMOS DDR is further increased when higher resistive load is applied. The proposed rectifier achieves the peak of PCE of 78.66% at P_{in} of -33dB for the resistive load of 500KΩ. The proposed design achieves similar high power conversion efficiency in comparison with conventional DTMOS DDR by using 3 times less RF input power level, which is critical for energy harvesting application.

ACKNOWLEDGEMENT

The authors acknowledge the financial support by Universiti Teknikal Malaysia Melaka's short term grant no. PJP/2015/FKEKK(5B)/S01424.

REFERENCES

- [1] M. Mahmoud, A. Abdel-Rahman, M. Abbas, et al, "Efficiency improvement of differential drive rectifier for wireless power transfer applications", *The 7th Int. Conf. on Intelligent Systems, Modelling and Simulation*, pp. 435-439, 2014.
- [2] F. Assaderaghi, D. Sinitsky, Parke, et al, "A dynamic threshold voltage MOSFET (DTMOS) for ultra-low voltage operation", *Electron Devices, IEEE Trans.*, vol. 4 no. 3, pp. 414-422, 1997.
- [3] S.S. Couhan, "CMOS integrated circuit for RF-powered wireless temperature sensor", Ph.D. dissertation, Dept. of Micro- and Nanoscience, Aalto Univ., Helsinki, Finland, 2015.
- [4] S. Oh, D.D. Wentzloff, "A -32dBm sensitivity RF power harvester in 130nm CMOS", *IEEE Radio Frequency Integrated Circuits Symposium*, pp. 483-486, 2012.
- [5] Y.C. Wong, P.C. Tan, M.M. Ibrahim et al, "Dickson charge pump rectifier using ultra-low power (ULP) diode for ban applications", *J. of Telecommunication, Electronic and Computer Engineering*, vol. 8 no. 9, pp. 5, 2016.
- [6] K. Kotani, A. Sasaki, T. Ito, "High-efficiency differential-drive CMOS rectifier for UHF RFIDs", *IEEE J. Solid-State Circuits*, vol. 44, no. 11, pp. 1-9, 2009.

Development of portable power generator by using dynamo

S.H. Johari*, Y.C. Chu, N. Abd Mutalib, S. Ahmad, M.F. Mohd Ab Halim, M. Zahari

Faculty of Engineering Technology, Universiti Teknikal Malaysia Melaka,
Hang Tuah Jaya, 76100 Durian Tunggal, Melaka, Malaysia.

*Corresponding e-mail: siti.halma@utem.edu.my

Keywords: Power generator; dynamo; boost converter, voltage regulator

ABSTRACT – This research presents the development of portable power generator by using dynamo. This project is used in emergency to generate power when no electric supply and no any renewable source example solar energy to charge any electronic device. In market, there have two types famous portable power generator which is power bank and solar power bank and both power bank have its pros and cons. The approach of power generator when generate the dynamo, the kinetic energy will be convert to electrical energy. The output voltage from dynamo is not stable because it is depending on the speed rotate of dynamo. In this development, Arduino UNO used as a microcontroller to control the pulse width modulation to a MOSFET, modern dc dynamo to generate electricity and DC-DC boost converter to step up and stabilize the output voltage from dynamo. The result for output voltage is 5V and it useful to charge small electronic devices.

1. INTRODUCTION

Nowadays we are living in an information technology (IT) world. Therefore at least one man has one mobile cell phone to make or accept calls, send or receive messages, play games, online shopping or act as Global Positioning System (GPS) to reach a destination. But, the battery storage for mobile cell phone is not enough as we need use it for few days without charging with plug, so a mobile power storage is needed when cell phone battery is not enough. Small scale mechanically driven electricity generators have continued to receive increasing attention as autonomous power source for low power electronic devices [1]. This principle can be applied when there is no electrical source. The instable output voltage from dynamo cannot directly use to charge electronic device. As to step up the electrical energy, a DC-DC boost converter need to construct [2]. In the DC-DC boost converter, a MOSFET device must receive pulse-width modulation to boost input voltage [3] as show in Figure 1. After boost convertor circuit, output voltage ripple will form and need to reduce [4] by adding the resistor and inductor to the circuit.

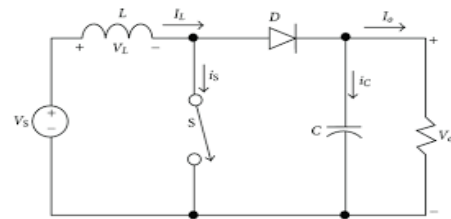


Figure 1 DC-DC boost converter circuit.

2. METHODOLOGY

The kinetic energy will convert to electrical energy when the hand crank dynamo tagged with number 1 start generated as soon as the pedal rotated as shown in Figure 2. The microcontroller Arduino Uno tagged with number 2 functions to control and give the signal of PWM to the gate driver labeled with number 3. Gate driver for MOSFET send the signal to active or close the gate pin of the MOSFET. After gate driver, the LC filter circuit labeled with number 4 is to reduce the ripple of the output voltage. After that, the voltage regulator tagged with number 5 function to maintain the voltage after a limit voltage. Lastly, the output to charge the device in range 5V can be connected at connector marked with number 6. Table 1 show the details of the hardware items used to develop a power generator whilst Figure 3 show the process flow of the system for charging.

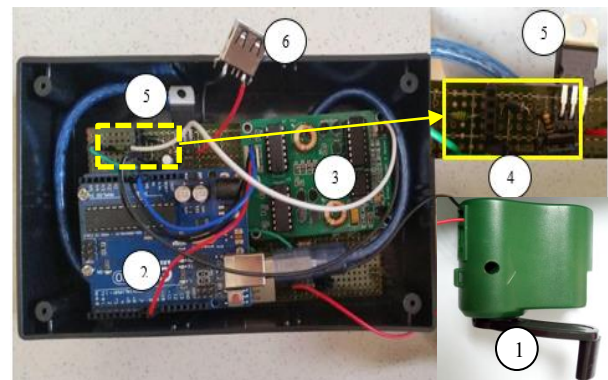


Figure 2 Hardware device.

Table 1 Hardware device items.

Item	Description
1	Hand crack dynamo
2	Microcontroller Arduino Uno
3	Gate driver
4	Filter circuit
5	Voltage regulator
6	Connector

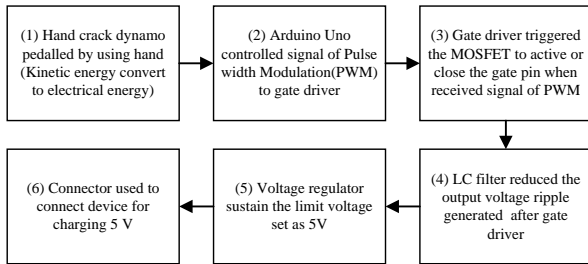


Figure 3 Power generator process flow.

3. RESULTS AND DISCUSSION

Figure 4 show the output voltage before LC filter increase linearly with the output voltage generated from dynamo. This graph demonstrates that the voltage before filter will keep increasing follow by the dynamo output voltage.

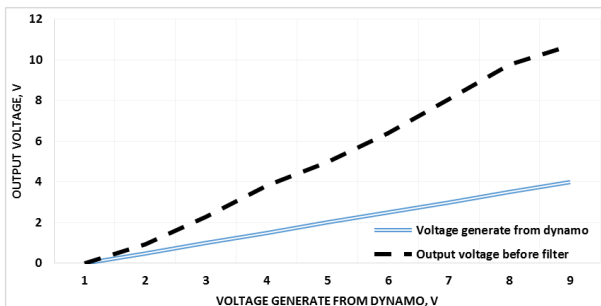


Figure 4: Dynamo output voltage vs output voltage before filter.

From Figure 5, the output voltage before voltage regulator increase linearly with output voltage measure at LC filter circuit. This graph represent that the output voltage will keep increasing follow by the input source.

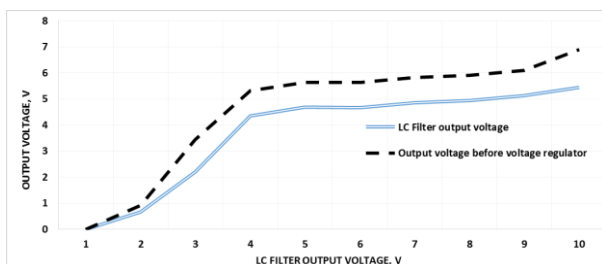


Figure 5 Output voltage vs output voltage before regulator.

Figure 6 shows the output voltage measured after voltage regulator also increase linearly with output voltage but stable at 5 V even the input voltage is risen up. This voltage regulator starts constant at 5 V when the LC filters output voltage at 4.9 V. Even the LC filter output voltage increase up to 5.45 V, the output voltage after regulator still remains stable.

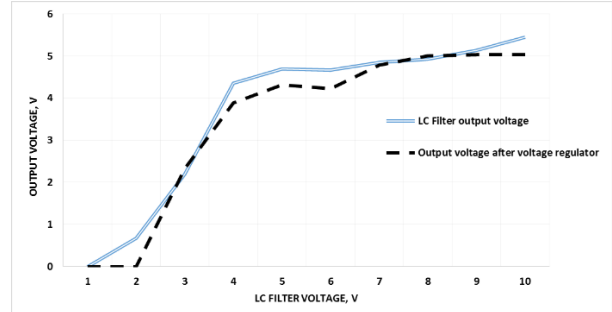


Figure 6 Output voltage vs output voltage after regulator.

4. CONCLUSIONS

After complete this development of power generator using dynamo, the maximum output voltage for the dynamo is 5.48V. The voltage produced instable and the LC circuit together with voltage regulator be located to improve voltage ripple and stabilize the output voltage to 5 V. Then, the desired output voltage 5 V able to use to charge small electronic devices.

ACKNOWLEDGEMENT

The author would like to acknowledge the Fakulti Teknologi Kejuruteraan (FTK) and Universiti Teknikal Malaysia Melaka (UTeM) for technical support.

REFERENCES

- [1] E. O'Riordan, D. Galayko, P. Basset, and E. Blokhina, "Complete electromechanical analysis of electrostatic kinetic energy harvesters biased with a continuous conditioning circuit," *Sensors Actuators, A Phys.*, vol. 247, pp. 379–388, 2016.
- [2] P. Tyagi, V. C. Kotak, and V. P. S. Singh, "Design high gain dc-dc boost converter with coupling inductor and simulation in psim," *IJRET Int. J. Research Eng. Technol.*, pp. 156–163, 2014.
- [3] Design an efficient DC-DC converter using the DS1875 PWM controller, <https://www.maximintegrated.com/en/app-notes/index.mvp/id/4332>.
- [4] C. Xia, Q. Geng, X. Gu, T. Shi, and Z. Song, "Input-output feedback linearization and speed control of a surface permanent-magnet synchronous wind generator with the boost-chopper converter," *IEEE Trans. Ind. Electron.*, vol. 59, no. 9, pp. 3489–3500, Sep. 2012.

Energy consumption analysis in engineering laboratory building

E.A. Thamer^{1,*}, B.T. Tee^{1,2}

¹⁾ Faculty of Mechanical Engineering, Universiti Teknikal Malaysia Melaka,
Hang Tuah Jaya, 76100 Durian Tunggal, Melaka, Malaysia.

²⁾ Centre for Advanced Research on Energy, Universiti Teknikal Malaysia Melaka,
Hang Tuah Jaya, 76100 Durian Tunggal, Melaka, Malaysia.

*Corresponding e-mail: thamer.e.anwer@gmail.com

Keywords: Energy consumption, lighting, laboratory

ABSTRACT – The growing demands for energy usage and better indoor environment quality has ignited interest in searching for modern solutions towards energy efficiency, electricity consumption and conservation in buildings. In this study an attempt is made to measure and evaluate the existing indoor parameters, which is focusing on the engineering laboratory building located in Mechanical Engineering Laboratory Complex (KMKM). The physical parameter conditions which include lighting and electricity consumption are then compared with the Malaysia Standard (MS 1525:2014). The results for this project provide illustrative pattern of indoor fluctuation and comfort parameters. The project also analyzed the impact of indoor lighting parameters on the comfort level of the occupants and identifies any changes in lighting effect. Based on the information and data collection, the total of the building energy consumption from lighting portion is then being estimated. In addition, the Building Energy Index is also being determined for each section in the building.

1. INTRODUCTION

The study of the building energy demand has become a topic of great importance [1][2], because of the significant increase of interest in energy sustainability. According to the circumstances it can be possible to determine the energy performance of a building through a calculation model starting from building known features (forward approach) or to assess the energy use from energy meters (inverse approach) [3].

The aim of this study is to analyze energy usage at Mechanical Engineering Laboratory Complex, using inverse approach, measured data for electricity and heating consumption is used. Collected information of buildings, and electricity and heating consumption is used to create a model. Creating a model of energy use helps in future building planning; it can provide useful information about most probable energy consumption for similar buildings, or predict energy use in different conditions. Also these models can be used to show impacts of possible energy savings measures and help in finding optimal way of reducing energy costs. It is also very important to have correct and reliable measured data. If a part of a building is leased to other users, there is necessity for calculating bills for each tenant [4]. There is increased interest in data error analysis and developing methods that can point out possible meters malfunction. Also, without correct measured data it is not possible to

monitor and prove benefits of applying energy saving measures for increasing energy efficiency [5].

The case study is conducted at the UTeM's Mechanical Engineering Laboratory Complex (KMKM) located at Taman Tasik Utama, Melaka. Figure 1 shows location and building orientation of KMKM which is at 2.2° 74'35.0" N 102.2° 82'31.3" E. KMKM is a building started operation on 2000 which consists of few block divided into five block which are A, B, C, D and E.

KMKM is a commercial building with 8243.49 m² floor area utilized as academic, purposes. The building consists of classroom, laboratories and staff's offices. Regarding with the current state of lighting system, there are two main type of lighting that used at this building which are 36 W T8 fluorescent lamps and 150 W metal halide lamps.

2. METHODOLOGY

Physical parameters measurement has been conducted in order to evaluate lighting through lux meter (center-337), and relative clamp meter (600A/600V). The lighting data was collected between 10 am to 12 pm and again 2 pm to 4 pm with the interval of 20 minutes between each reading. The measurements were done at five sections (A, B, C, D and E) of the KMKM building.



Figure 1 Map of the KMKM building.
(Source: Googlemap).

3. RESULTS AND DISCUSSION

Figure 2 shows the total number of readings as recorded by using lux meter in each section of the building. Readings were recorded in one whole day with 20 minutes interval between each reading. The light meter provides a simple and effective method to determine the actual lighting level that is being

transmitted. It is useful to compare the actual level with proposed or recommended levels for certain activities or area. Lighting inventory in Section A and B consumed less watts followed by Section D. Section C consumed maximum watts compare with other sections. The lighting average is same for section A, B, C, D and E in morning and afternoon.

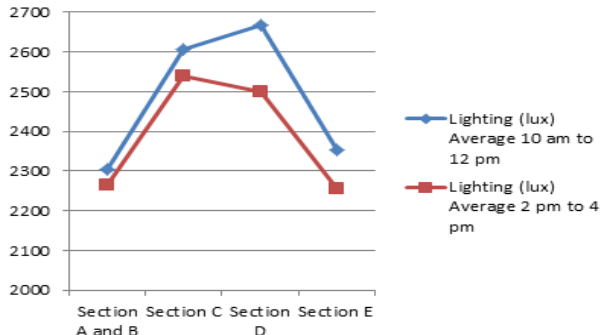


Figure 2 Overall lighting (lux) measurement.

Clamp meter is used to measure total current flowing in the conductor through the probe, which depends on the relationship of phase current vector [6]. It is useful to compare our real level with proposed or recommended levels for certain activities or area. Total energy consumed in Dynamic laboratory (section E) was the highest followed by Computer design studio (section D) compare with other areas. Figure 3 show the comparison between consumed watts in each section for hourly, daily, weekly and monthly.

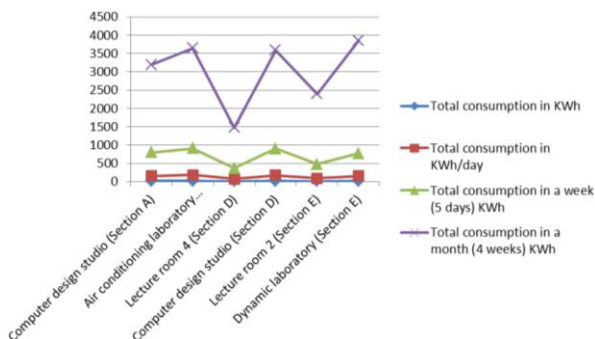


Figure 3 Each section total consumption.
(per day/per week/per month)

4. CONCLUSION

Referring to the results of the measured physical parameter, most of the sections of the building do not achieve the acceptable lighting illumination as recommended by MS 1525:2014. As there is no sub-metering devices for lighting portion being installed in the case study building, assumptions have been made to estimate the energy consumption in the building from the lighting portion. The overall Building Energy Index (BEI) of the building is 85.40 kWh/m²/yr.

REFERENCES

- [1] J.L.S. Chong, A. Husain, B.T. Tee, "Simulation of airflow in lecture rooms", Proc. of the AEESAP International Conference, 2005.
- [2] R. Hywel, B.T. Tee, M.Y. Arifin, C.F. Tan, C.K. Gan, C.T. Chong, "ACMV energy analysis for academic building: a case study", IOP Conference Series: Materials Science and Engineering, vol. 88(1), 2015.
- [3] I. Sartori, A. Napolitano, and K. Voss, "Net zero energy buildings: A consistent definition framework," *Energy and Buildings*, vol. 48, pp. 220-232, 2012.
- [4] S. Kelly, D. Crawford-Brown, and M. G. Pollitt, "Building performance evaluation and certification in the UK: Is SAP fit for purpose?," *Renewable and Sustainable Energy Reviews*, vol. 16, pp. 6861-6878, 2012.
- [5] A. Sretenovic, "Analysis of energy use at university campus," 2013.
- [6] P. R. Hutt and S. Day, "Electronic electricity meters," ed: Google Patents, 1990.

Study on the effect of feed water flow rate on the steam turbine speed in the experimental vehicle

S.G. Herawan^{1,2}, K. Talib^{1,*}, M.M. Tahir^{1,2}, S. Anuar^{1,2}, A. Putra^{1,2}, M.S. Rahman^{1,2}

¹⁾ Faculty of Mechanical Engineering, Universiti Teknikal Malaysia Melaka, Hang Tuah Jaya, 76100 Durian Tunggal, Melaka, Malaysia

²⁾ Centre for Advanced Research on Energy, Universiti Teknikal Malaysia Melaka, Hang Tuah Jaya, 76100 Durian Tunggal, Melaka, Malaysia

*Corresponding e-mail: helmy2127@gmail.com

Keywords: Waste heat recovery, exhaust heat, steam turbine mechanism

ABSTRACT –For a vehicle using internal combustion engine (ICE), the waste energy produce by exhaust can be harness by implementing heat pipe heat exchanger in the automotive system. In this study, the fluid used is water, thus converting the system to steam turbine mechanism. Water will absorb heat from exhaust, converting the fluid into steam and thus drive the turbine that coupling with generator. The paper will explore the effect of feed water flow rate on the steam turbine speed. The experiment is conduct in order to determine the best flow rate used to achieve optimum steam turbine speed.

1. INTRODUCTION

The issue of global warming has pushed the effort of researchers, not only to find alternative renewable energy, but also to improve the machine's efficiency. This includes the utilization of waste energy into useful energy. The energy from the automotive exhaust can be harness by implementing heat pipe heat exchanger in the automotive system. In order to maximize the amount of waste energy that can be turned to useful energy, the used of appropriate fluid in the heat exchanger is important. Water is used as the fluid, thus converting the system to steam turbine mechanism.

It has been identified in [1] that the temperature of the exhaust gas varies depending on the engine load and engine speed. As the engine speed increases, the temperature of the exhaust gas will also increase. Engine speed, vehicle speed, throttle angle, and exhaust temperature are identified as the measured parameter of steam turbine speed performance [2,3]. In this study, water pump is used in order to produce constant flow of water through the helical copper coil. Note that, the study is done from real condition and on the real road track. Therefore, all the measured parameters are in full dynamic condition, meaning that none of the parameters was under control. However, there is one parameter that can be set in control, which is the feed water flow rate. In order to determine the exact water flow rate that can give optimum performance, an experiment need to be done.

2. METHODOLOGY

The experiment was performed on a Toyota vehicle having 1.6 liter in-line four-cylinder gasoline engines. The detail of running this experimental vehicle can be found in [4]. Table-1 shows the specification of the test

engine. A schematic diagram of the experimental setup is shown in Figure 1.

Table 1 Specification of the test engine.

Type	Specification
Valve train	DOHC 16 valves
Fuel system	Multi point fuel injection
Displacement	1587 cc (in-line)
Compression ratio	9:4:1
Bore	81 mm
Stroke	77 mm
Power	112Hp @ 6600 rpm
Torque	131Nm @ 4800 rpm

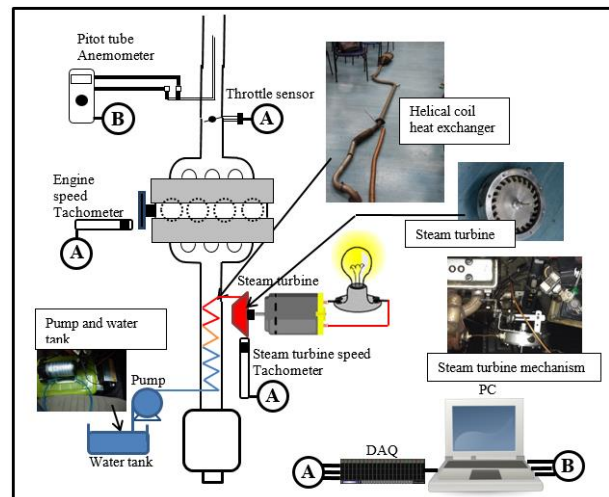


Figure 1 Schematic layout of the experimental setup of waste heat recovery mechanism.

To determine the optimum feed water flow rate for helical coil heat exchanger, three tests were being conducted using the experimental vehicle by varying the feed water flow rate at 100 ml/min, 160 ml/min, and 270 ml/min. The experiment is design to run in six (6) rounds as shown in Figure 2.

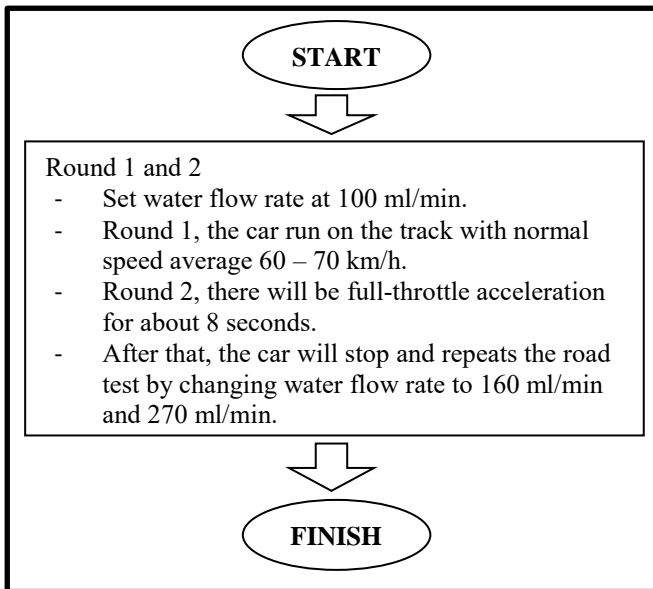


Figure 2 Flowchart of the road test.

3. RESULT AND DISCUSSION

Figure 3, Figure 4 and Figure 5 show the steam turbine speed against the exhaust temperature at 100 ml/min, 160 ml/min, and 270 ml/min respectively. Feed water flow rate of 100 ml/min produced a steam turbine speed in the range of 1000 rpm to 14000 rpm in the normal driving test, and can reached up to 25000 rpm in the full throttle test (Figure 3). For 160 ml/min produced 8000 rpm to 30000 rpm in the normal driving test and up to 33000 rpm in the full throttle test (Figure 4). While, 270 ml/min generated 3000 rpm to 15000 rpm in the normal driving and reached up to 25000 rpm in the full throttle test (Figure 5).

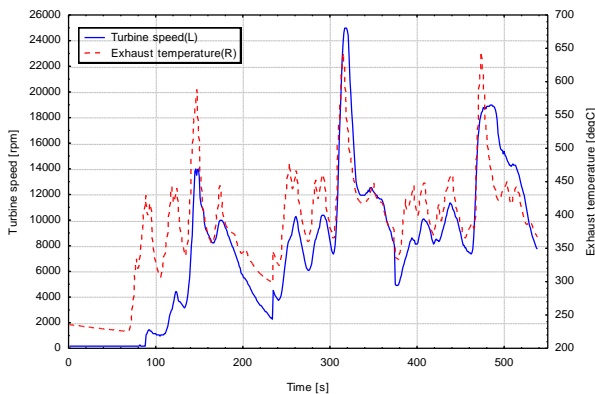


Figure 3 Steam turbine speed against exhaust temperature at 100 ml/min.

4. CONCLUSION

By comparing the three feed water flow rates, the flow rate of 160 ml/min had an optimal result for steam turbine speed. For this helical coil heat exchanger in the experimental vehicle, this feed water flow rate gave a proper mass flow rate for the available latent heat, which could boost all of the feeding water into steam.

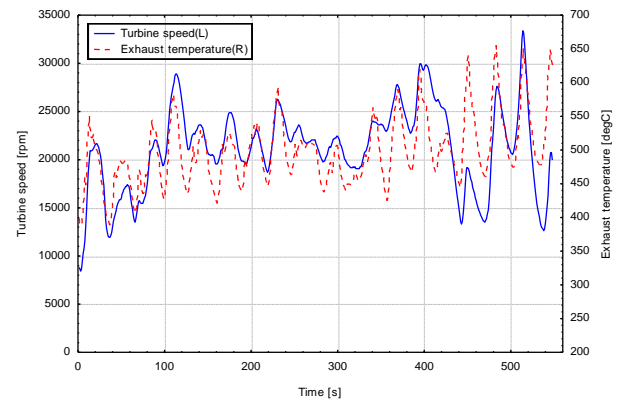


Figure 4 Steam turbine speed against exhaust temperature at 160 ml/min.

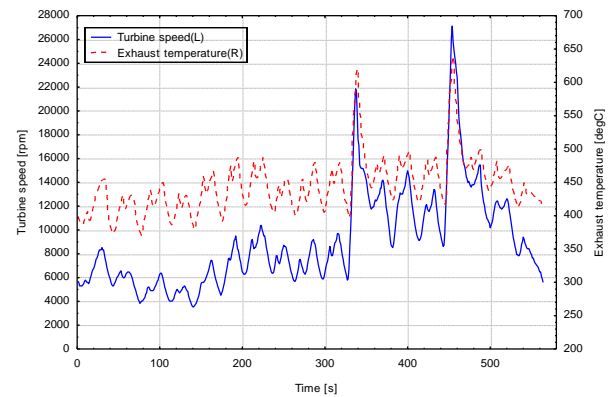


Figure 5 Steam turbine speed against exhaust temperature at 270 ml/min.

ACKNOWLEDGEMENT

Grant no.: FRGS/2/2014/TK06/FKM/02/F00236.

REFERENCES

- [1] Z. Peng, T. Wang, Y. He, X. Yang & L. Lu, "Analysis of environmental and economic benefits of integrated Exhaust Energy Recovery (EER) for vehicles", *Applied energy*, vol. 105, 238-243, 2013.
- [2] S.G. Herawan, A.H. Rohhaizan, A.F. Ismail, S.A. Shamsudin, A. Putra, M.T. Musthafah, & A.R. Awang, "Prediction on Power Produced from Power Turbine as a Waste Heat Recovery Mechanism on Naturally Aspirated Spark Ignition Engine Using Artificial Neural Network", *Modelling and Simulation in Engineering*, vol. 2, 2016.
- [3] K. Talib, S.G. Herawan, M.M. Tahir, A. Putra & S.A. Shamsudin, "Study on waste heat recovery from exhaust gas spark ignition (SI) engine using steam turbine mechanism", *MATEC Web of Conferences*, vol. 90, p. 01057, 2017.
- [4] S.G. Herawan, A.H. Rohhaizan, A. Putra, & A.F. Ismail, "Prediction of waste heat energy recovery performance in a naturally aspirated engine using artificial neural network", *ISRNN Mechanical Engineering*, 2014.

Investigation on waste materials as thermal insulation for building

I.M. Naji¹, M.Z. Akop^{1,2,*}, B.T. Tee^{1,2}, M.A. Salim^{1,2}, M.R. Mansor^{1,2}, A.R. Dullah^{1,2}, A.M. Saad^{1,2}, M.A.M. Rosli^{1,2}, Y.M. Arifin^{1,2}

¹) Faculty of Mechanical Engineering, Universiti Teknikal Malaysia Melaka,
Hang Tuah Jaya, 76100 Durian Tunggal, Melaka, Malaysia

²) Centre for Advanced Research on Energy, Universiti Teknikal Malaysia Melaka,
Hang Tuah Jaya, 76100 Durian Tunggal, Melaka, Malaysia

*Corresponding e-mail: zaid@utem.edu.my

Keywords: Thermal insulation, waste materials, reconfigurable model house.

ABSTRACT - Wall insulation is one of the most important things that can keep the surrounding temperature of the homes or any building suitable. It helps in maintaining the human comfort. The aim of this research is to study coconut coir and cellulose as a potential waste material for thermal insulator. This research tested these two materials and three existing thermal insulator materials in a reconfigurable model house Marcraft GT-7500 for comparison. The internal and external temperatures were measured at selected location for internal and external heat loads condition. The temperature measurement leads for better thermal conductivity to conventional insulation.

1. INTRODUCTION

The relation between human and heat energy must be addressed. This relation is known as thermal comfort. It is “that condition of mind which expresses satisfaction with the thermal environment when the body functions well”. Human comfort is achieved when the surrounding circumstances are appropriate in terms of temperature. Appropriate conditions avoid the person feel cold or too hot with a body temperature of around 37°C and skin temperature of 32-33°C [1]. The body temperature in a wide range of climates could be maintained in various ways [2].

Generally, Malaysia climate is hot and humid. To achieve the thermal comfort on human body, cold or moderate air must be provided by using air-conditioning devices or any other cooling equipment. There is an important thing should be considered, it's about the keeping of good atmosphere and save the energy in the building. Increase in the cost of energy consumption in the building emphasizes to find immediate solution and work to energy conservation even in countries have the oil producer. In building sectors, there is an effective way to save the energy by using thermal insulation to keep the comfort level. Thermal insulation is one of the main material used to conserved energy [3]. Maintain the inside temperature of the building will generally reduce usage of energy. In fact, insulation will also reduce the noise and give more quality and comfort to human in the buildings. The capability of insulation material is measured by thermal conductivity (k) where its shows the ability of specified material to conduct heat [4].

The aim of this study is to find thermal insulation in a moderate price and give a good performance with high effectiveness. The focus will be on waste materials that could be as alternative potential thermal insulators. Coconut coir and cellulose will be taken as example for this study. Coconut coir, cellulose and others current insulators compared in terms of its value of k . In addition, the experiment was conducted in order to prove the efficiency of coconuts coir and cellulose fibre as alternative thermal insulations.

2. METHODOLOGY

The insulation material will be formed in 428mm x 132mm x 15mm thickness shape and inserted into the 5 side cavities (except back side cavities). The materials are coconut coir and cellulose and three of common thermal insulations. These materials are tested in mini model house Marcraft GT-7500 as shown in Figure 1.



Figure 1 The reconfigurable model house Marcraft GT-7500.

Firstly, the all insulator made from different material will be tested by applying external heating from 1000W spot light at the side wall. The ambient temperature and temperatures inside the mini house will be measured by using thermocouples. The same insulator will be tested by applying internal heating generated by bulb inside the model house.

The duration of experiment is 20 minutes and the temperatures are measured at 5 interval times i.e. 0, 5th, 10th, 15th and 20th minutes.

3. RESULTS AND DISCUSSION

Table 1 shows the inside and outside average temperature of the mini house in the 20th minute for the external heating case.

Table 1 Inside and outside average temperature for external heating case.

Material	Temperature at 20 th minutes, °C	
	In	Out
Polystyrene	31.3	36.6
Cotton	30.7	36.6
Fiberglass	31.4	36.5
Cellulose	31.3	35
Coconut coir	31.2	36.2

Table 2 below shows the values of the total heat transfer rate, Q, R-value and heat flux for all material selected. These values were obtained from external heating case of the experiment.

Table 2 Parameters and variables for external heating case.

Material	Parameters / variables			
	k, W/m. K	Q _{total} W	R _{value}	Heat flux W/m ²
Polystyrene	0.34	3.359	0.108	48.1622
Cotton	0.029	2.683	0.153	38.468
Fiberglass	0.04	3.368	0.1056	48.296
Cellulose	0.04	3.523	0.0732	50.511
Coconut coir	0.043	3.457	0.1	49.563

R-value is known as the thermal effectiveness of materials. It depends on the thermal conductivity and refers to the effectiveness of material as thermal insulation. When the value of k is low, R-value should be high and it show the material is good as thermal insulation. In internal heating cases, there are a different concept of the experiment where internal heat source applied in the model house. The average inside and outside temperature for this cases shown in Table 3.

Table 3 Inside and outside temperature values for internal heating.

Material	Temperature at 20 th minutes, °C	
	In	Out
Polystyrene	36	29
Cotton	37	29.6
Fiberglass	36	29.3
Cellulose	33	29.6
Coconut coir	36	30.4

In a Table 4 below shows the values of the total heat transfer rate, Q, R-value and heat flux for all material selected. These values were obtained in cases of internal heating.

Table 4 Parameters and variables for internal heating case.

Material	Parameters / variables			
	k, W/m. K	Q _{total} W	R _{value}	Heat flux W/m ²
Polystyrene	0.34	3.218	0.201	16.833
Cotton	0.029	2.083	0.311	10.928
Fiberglass	0.04	3.307	0.195	17.350
Cellulose	0.04	3.864	0.167	20.273
Coconut coir	0.043	3.445	0.188	18.074

4. CONCLUSION

The main aim of the study is to determine the effectiveness and performance of coconut coir and cellulose as thermal insulation materials. They are considered to be as a competent thermal insulation material as the value of their thermal conductivity below than 0.1 W/m. K which is the range of possible insulation. Moreover, the total of heat transfer and the effectiveness was in a close gap to the other common thermal insulation. These results make coconut coir and cellulose as acceptable thermal insulations.

REFERENCES

- [1] K. Parsons, "Human Thermal Environments: The Effects of Hot, Moderate, and Cold Environments on Human Health, Comfort, and Performance," 3rd edition, CRC Press 2014.
- [2] R. McIlveen, "Fundamentals of Weather and Climate," Oxford University Press, 2010.
- [3] S. Mishra, D.J.A. Usmani, and S. Varshney, "Energy saving analysis in building walls through thermal insulation system", *International Journal of Engineering Research and Applications*, vol. 2(5), pp. 128-135, 2002.
- [4] M.I. Pryazhnikova, A.V. Minakova, V.Y. Rudyaka, and D.V. Guzeib, "Thermal conductivity measurements of nanofluids", *International Journal of Heat and Mass Transfer*, vol. 104, pp. 1275-1282, 2017.